Heliyon 7 (2021) e08520

Contents lists available at ScienceDirect

Heliyon

journal homepage: www.cell.com/heliyon

Research article

Assessment of seismic hazards in Yemen

Mohammed Alrubaidi [a], Mohammed S. Alhaddad [b], Sulaiman I.H. Al-Safi [c], S.A. Alhammadi [d,*], Abobaker S. Yahya [b], Aref A. Abadel [b]

[a] Department of Civil Engineering, Emirates International University, Sana'a, Yemen
[b] Department of Civil Engineering, King Saud University, Riyadh, Saudi Arabia
[c] Department of Civil Engineering, Sana'a University, Sana'a, Yemen
[d] Vice Rectorate for Facilities and Operation, Princess Nourah Bint Abdulrahman University, Riyadh, Saudi Arabia

ARTICLE INFO

Keywords:
Seismic hazard
PSHA
Maximum magnitude
Rupture characteristic
SA
Yemen
PGA

ABSTRACT

The seismic hazard analyses for Yemen have attracted the attention of researchers during the last two decades. However, the studies are limited and mainly use deterministic or approximate conventional probabilistic approaches. The conclusions drawn from these studies do not fit with current seismic design codes (International Building Code). This article presented the method and findings of a probabilistic seismic hazard assessment for Yemen in accordance with current seismic design building regulations. All the data sources, available nationally and internationally, were utilized in compiling earthquake database by covering the recent records and the seismic activity maps of the study region. The study area was regionalized to 11 seismotectonic area sources on the basis of the seismicity maps and available tectonic maps. On the analytical side, the earthquake recurrence analysis was evaluated for each source, and logic tree concept was used to model the seismic sources that may have significant effect on seismic hazard evaluation of Yemen as a combination of area and line sources. A probabilistic forecasting model was formulated, appropriate ground motion attenuation relationships were used, and seismic hazard contour maps were developed for the entire Yemen area. The maps present dense contours of peak ground accelerations and short and long period spectral accelerations for different return periods. The highest predicted seismic hazard is found in Dhamar City. This study provides basic and essential requirements that will be valuable in developing advanced seismic design criteria for Yemen.

1. Introduction

Earthquake is one of the most devastating natural hazards, causing enormous loss of life and property throughout history. Destruction is caused by the collapse of buildings and compounded by landslides, floods, tsunamis, and fires arising due to earthquakes. The Republic of Yemen has a long history of seismic and volcanic activity related to its location in the southwestern Arabian Peninsula and eastern Africa (Somalia, Djibouti, and Eritrea), part of the active Arabian tectonic plate. Active spreading of the Arabian plate from the African plate along the Red Sea, Gulf of Aden, and Afar depression produces shallow intrusive magmatic activity near the Arabian plate's southwestern border, which is an important factor in the control of seismic activity in Yemen (Figure 1) [1]. Seismotectonic settings in and around Yemen strongly indicate the possibility of major earthquakes, especially in Dhamar and along the Arabian plate borders, which may inflict considerable damage to Yemeni structures. The most efficient method to reduce earthquake-related catastrophes is to better design and construct buildings. The current research emphasizes the need of measuring ground motion parameters in Yemen for earthquake-resistant design and seismic safety evaluation. Aleatory variability and epistemic uncertainty are two sources of unpredictability in seismic hazard assessment. The current study utilizes probabilistic seismic hazard analysis (PSHA) in conjunction with CRISIS 2007 software [2]. Aleatory variability due to random effects is directly included in PSHA calculations to determine the annual exceedance frequencies of different ground motion amplitudes. This process is conducted by integrating the relevant probability density functions within a specified range of standard deviations. To address epistemic uncertainty, contemporary PSHA studies use the "logic tree" technique.

Several studies have been conducted in various regions of the Arabian Peninsula to assess the seismic hazard. The first study for Yemen was conducted by Al-Dafiry [3], who used ground motion models to estimate peak ground acceleration (PGA) and proposed a seismic zonation map for Yemen to be used as a basis for seismic design based on the Uniform

* Corresponding author.
E-mail address: saalhammadi@pnu.edu.sa (S.A. Alhammadi).

https://doi.org/10.1016/j.heliyon.2021.e08520
Received 23 September 2021; Received in revised form 1 November 2021; Accepted 29 November 2021

Figure 1. Cenozoic tectonic setting of the Arabian plate. Reproduced from ref. [1] with the permission of Springer Nature Ltd, 2021.

Building Code (UBC 97) [4]. Al-Suba [5] provided a peak horizontal ground acceleration map (contours) only for the western Yemen region. Mohindra et al. [6] utilized the PGA for a 10% probability of exceeding in 50 years (return period 475 years) for seismic hazard analysis in Yemen by using the same model that Al-Haddad et al. [7] used to evaluate seismic hazard and design criteria in Saudi Arabia. Al-Haddad et al. [7] applied these attenuation equations for all seismic sources in the region of the Arabian Peninsula, including Yemen, in creating seismic hazard and design standards for Saudi Arabia. According to Mohindra et al. [6], their study has some limitations and shortcomings, such as they do not consider epistemic uncertainty in all of the inputs to the hazard assessment, which is typically incorporated using the logic tree approach, and aleatory uncertainty in PGA-intensity conversion. The attenuation relations used in the study by Mohindra et al. [6] may have some regional biases.

Many studies have been conducted on Yemen's neighbor countries, such as the Kingdom of Saudi Arabia and Oman's Sultanate. Saudi Arabian researchers used numerous ground motion prediction models to determine PGA and velocity for stiff soil and a 10% chance of exceeding these values in 100 and 50 years [8, 9, 10, 11, 12, 13, 14, 15, 16]. Many venerable studies have served as a foundation for all subsequent research on the Arabian Peninsula [17, 18, 19, 20, 21, 22, 23, 24]. Numerous studies have been conducted for the Sultanate of Oman using the regional seismic hazard model, where many of them have been performed by El-Hussein et al. The most famous was in 2012 [24], which contains the spectral amplification maps for earthquake features on the ground surface in the Sultanate of Oman are provided over a 475-year return period.

Previous studies conducted in Yemen were few and did not develop a technique for providing seismic maps relevant to the design of seismic buildings. This study focuses on the sources of earthquakes and the impact of earthquakes on all areas of the country and derives the uniform hazard spectrum (UHS) for Yemen by using CRISIS 2007 software [2] via a logic tree framework on the basis of rigorous data from multiple resources and attenuation relationships. Other important steps are detailed in the following sections for issuing useful maps to design earthquake-resistant buildings that were previously unavailable. This article presents the method and findings of a probabilistic seismic hazard assessment for Yemen in accordance with current seismic design building regulations, which are the International Building Code (IBC) for seismic design [25] and the Minimum Design Loads and Associated Criteria for Buildings and Other Structures, (ASCE/SEI 7–16) [26]. No building code is available for Yemen. The IBC [25] code, which is based on the design of buildings by selecting values of 0.2-s spectral response acceleration (Ss in percent g) and 1.0-s spectral response acceleration (S1 in percent g) (5% of critical damping), is used. These values are not used in previous Yemen studies.

On the basis of data from various worldwide and local seismic catalogs from 112 to 2021 AD, the earthquake catalog for Yemen and the surrounding regions was obtained and revised with magnitudes (M) $\geq$ 4.0 (Figure 2). The catalog was declustered to remove dependent events,

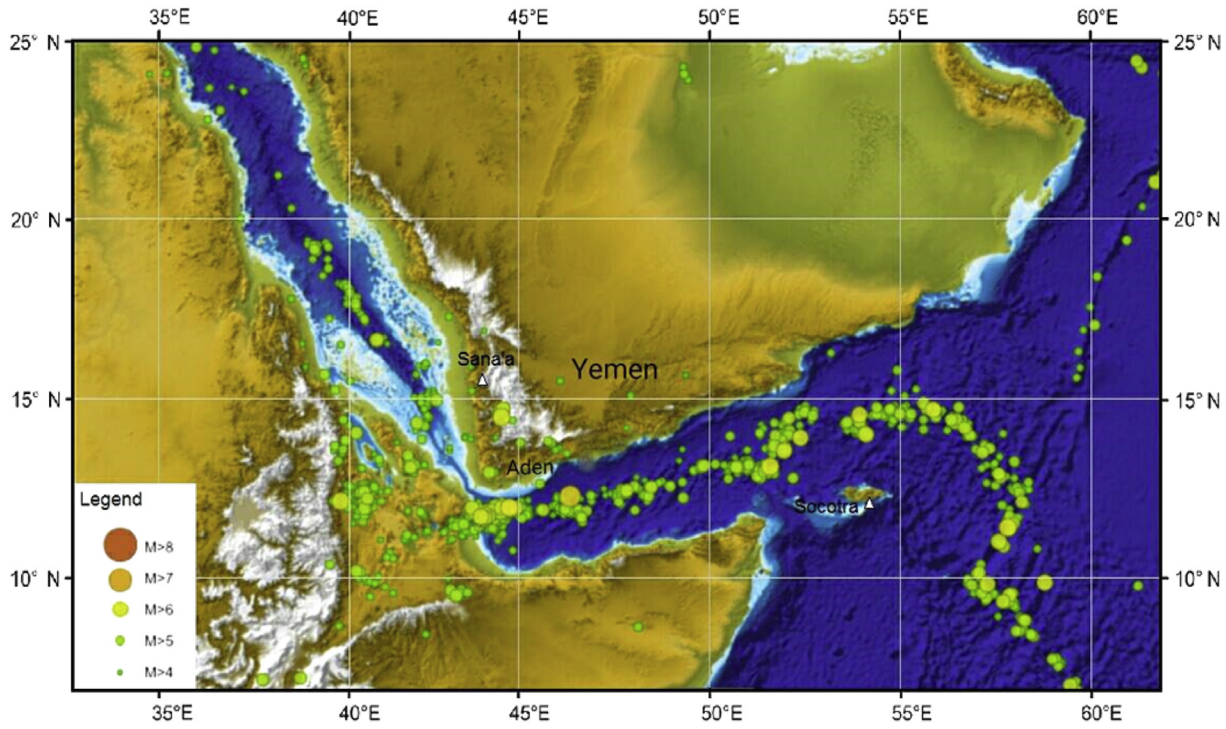

Figure 2. Distribution of epicenters of shallow earthquakes (depth 10–30 km) and M ≥ 4.0 in and around Yemen that have occurred up to August 2021 (compiled from collected available earthquake catalogues). Reproduced from ref. [31] USGS.

and duplicates were removed (aftershocks, foreshocks, and earthquake swarms). A large number of earthquake faulting mechanisms for Yemen were collected from local and international sources to help define a representative seismotectonic model. Establishing a representative focal mechanism for each seismic source by using the collected focal mechanisms is feasible.

This research identified a total of 11 seismic sources (Table 1) on the basis of the locations of the seismic events in Yemen. Sets of recurrence parameters (β, λ, and M_{max}) are calculated for each seismic source by using the compiled earthquake catalog. Alternative ground motion scaling equations for rock are utilized to provide damped spectral acceleration values of 5% for a variety of spectral acceleration (SA, 0.2, 1.0 s) and PGA for return periods (475, 2475 years) (equivalent to 2% and 10% probability of exceedance in 50 years, respectively).

2. Tectonic setting

As a consequence of the spreading process of the Arabian Plate from the African Plate and the stages of opening up the Red Sea and Gulf of Aden, the tectonic setting of the Republic of Yemen is significantly affected by the tectonic setting of the Arabian Plate. The tectonic setting of the Red Sea and Gulf of Aden had a significant impact on the region's tectonic setting during the stages of forming the Red Sea, which has distinctive fault systems and weakness zones in dry and submerged places. The Arabian Peninsula is divided into two adjacent tectonic regions: the internal stable zone, which is composed of basement rocks covered in sediment, and the outer mobile belt region. The basement rocks of the interior area have undergone many phases of melting and alteration, resulting in the formation of numerous fault systems [27]. The exterior movable area was influenced by the uplift of the western Arabian Peninsula and the division of east Africa into several pieces. Lava extruded via faults and fissures to cover the Precambrian Basement and overlying layers due to the separation. This process resulted in the disintegration of mountains into many pieces and the development of various fault systems, with vertical displacement between blocks reaching 2000 m in certain places. Some of these faults run north–northwest parallel to the Red Sea axis, and others run east–northeast parallel to the Gulf of Aden axis. The faulted Graben and Eastern Yemen Horst, which include the coastal plain and Yemen's central highland, are thought to represent the earliest indications of the development of the Red Sea Rift [27].

As illustrated in Figure 3, three major orientations for faults influence the rocks of the Republic of Yemen [28].

2.1. Fault group Northwest–Southeast

This group is a common category of faults that are distinguished by their large displacement. It is abundant in the western areas parallel to the Red Sea Rift region.

2.2. Fault group East–West

This group of faults is less widespread and concentrated in the south, such as the Saber Fault. It is distinguished by its large displacement, which forms a series of highlands and depressions, particularly between Taiz and Ibb.

2.3. Fault group Northeast–Southwest

This group of faults is uncommon and may have formed near the end of the Tertiary period. It is based on recent formulations that affect the rocks of the Yemeni Plateaus. In addition to the fault groups, two large tectonic provinces are formed, which are considered to be part of Yemen's main tectonic setting [27].

2.3.1. Central depression (basin) province

This province is a north northwest–south southeast direction that extends southward to Hadramawt. It constitutes many secondary tectonic basins from south to north, such as Qataba, Yarim, Dhamar, Ma'bar, Amran, Jawf, and Sa'dah basins. This province tectonic setting is considered the weakest [29].

Table 1. Seismic sources of seismotectonic source model for the PSHA*.

Zone No	Name	Zone Corners		
		Designation	Coordinates	
1	Sheba Ridge	A1	56.4 N,	10.2 E
		B1	56.5 N,	12.4 E
		C1	58.5 N,	11.7 E
		D1	59.0 N,	8.5 E
2	East Sheba Ridge	A2	54.6 N,	14.0 E
		B2	54.0 N,	16.1 E
		C2	59.3 N,	13.5 E
		C1	58.5 N,	11.7 E
3	Gulf of Aden	A3	41.5 N,	12.0 E
		B2	54.0 N,	16.1 E
		A2	54.6 N,	14.0 E
		B3	44.3 N,	10.3 E
4	East Rub al Khali Arabian Shield	A4	48.9 N,	18.5 E
		B4	52.0 N,	19.2 E
		B2	54.0 N,	16.1 E
		C4	50.0 N,	14.9 E
5	North Rub Al-Khali Arabian Shield	A5	45.2 N,	17.3 E
		A4	48.9 N,	18.5 E
		B5	49.6 N,	16.6 E
		C5	45.7 N,	15.6 E
6	Yemen Southern Arabian Shield	C5	45.7 N,	15.6 E
		B5	49.6 N,	16.6 E
		C4	50.0 N,	14.9 E
		A6	46.1 N,	13.6 E
7	Yemen North western Arabian Shield	A7	43.4 N,	15.8 E
		A5	45.2 N,	17.3 E
		A6	46.1 N,	13.6 E
		B7	42.1 N,	12.6 E
8	Yemen Southwestern Arabian Shield	A8	42.3 N,	17.9 E
		B8	44.5 N,	18.5 E
		A5	45.2 N,	17.3 E
		A7	43.4 N,	15.8 E
9	Red Sea-Al Darb	A9	38.8 N,	18.2 E
		B9	41.4 N,	19.5 E
		A7	43.4 N,	15.8 E
		B7	42.1 N,	12.6 E
10	African Southwestern Red Sea	A11	39.1 N,	11.0 E
		A10	39.5 N,	14.6 E
		B10	41.1 N,	15.2 E
		B7	42.9 N,	12.6 E
11	East African Rift	A11	39.1 N,	11.0 E
		A3	41.5 N,	12.0 E
		B3	44.3 N,	10.3 E
		B11	39.9 N,	8.6 E

* The region corners are designated A, B, C, in clockwise order in the Table with A being in the north-west corner of the region.

2.3.2. Jawf valley depression (basin) province

This province is a west northwest–east southeast direction that formed during the Jurassic period. It is connected to Ramlat Sabatayn basin in the east.

3. Seismicity of Yemen

Yemen has been characterized by seismic activity throughout history due to its location in the southwestern part of the Arabian Peninsula, near to the active seismic area of the Red Sea and Gulf of Aden, where the bulk of activity occurs. Seismic activity is associated with volcanism. In accordance with the tectonic setting and seismic data, Yemen has a low to moderate seismicity [30]. The first known earthquake occurred in the desert of Sheba near Ma'rib in 742, and the Sa'dah 1941 earthquake is regarded as the first damaging earthquake in modern history. Yemen may be split into two seismic zones: maritime seismic zone and continental seismic zone.

This research utilizes five sources of seismic data as follows:

a) Ambraseys (1988) [18] from 112–1963 AD.
b) United States Geological Survey (USGS) [31] (Preliminary determination of epicenters [PDE] and earthquake data report [EDR]) - for the period 1964–2021.
c) The European Mediterranean Seismological Center (EMSC) [32]: 1990–2021.
d) The International Seismological Center (ISC) [33]: 1964–2021.
e) National Seismological Observatory Center (NSOC), Dhamar, Yemen [34] - for the period 2000–2015.

The duration of seismic data gathering is split into three periods.

a) Historical - for the period 112–1964.
b) Instrumental - for the period 1965–1985.
c) Recent Seismicity-for the period 1986–2021.

3.1. Historical seismic activity - for the period 112–1963

The historical seismic activity of Yemen is based on books and papers written at a time when seismic instruments were unavailable. It was primarily gathered from inscriptions, chronicles, archives, travelers, and witnesses to the events. Historical seismicity is characterized by medium-magnitude earthquakes that occur with some regularities in coastal and inland regions. The majority of them were followed by long aftershocks, indicating that they were caused by volcanism. Table 2 contains a list of historical earthquakes in Yemen from 742–1900 [30], compiled by Ambraseys and Melville. The Sa'dah 1941 earthquake was the most destructive large earthquake that occurred during this time period. The seismotectonic map of Yemen (epicentral distribution for 742–1899 [34] and the main tectonic trends, volcanic necks, and hydrothermal spring distribution) are shown in Figure 4. An earthquake with a magnitude of $M = 5.8$ was felt from Jizan to Al-Mukalla on January 11, 1941, preceded by a foreshock on January 9, 1941. Several settlements were destroyed at Razih, with only minor casualties. Landslides blocked the road at the head of the Razih Valley, causing damage in Kuhlan and Hajjah. Strong aftershocks were reported from Hudaydah, Bayt Al-Faqih, and other locations on February 4 and February 23, 1941, up until the second week of March. These aftershocks killed 1200 people, injured 200, destroyed many houses, and damaged approximately 1400.

3.2. Instrumental seismic activity - for the period 1964–1985

During this time period, 239 seismic events with a magnitude of ≥ 4.0 occurred between 10 and 30 km. The majority are located along spreading ridges (the Red Sea and Gulf of Aden), and a low level of seismicity characterized by small to moderate-sized events occurs within the Arabian plate within 200–300 km of the Red Sea's axis in Yemen and extends southward into adjacent areas. The Dhamar 1982 earthquake was the most destructive large earthquake that occurred during this time period.

An earthquake of magnitude $M = 6.3$ [31] struck the governorate of Dhamar on December 12, 1982, at 12:12 PM. The epicenter of the earthquake was located 10 km southeast of Ma'ber, with a hypocenteral depth range of up to 5 km. The epicenter zone was located in the Jahran Basin, approximately 70 km south of Sana'a and 17 km N of Dhamar, at latitude 14.7N and longitude 44.37E. The earthquake was preceded by minor foreshocks that occurred within seconds of the main shock and

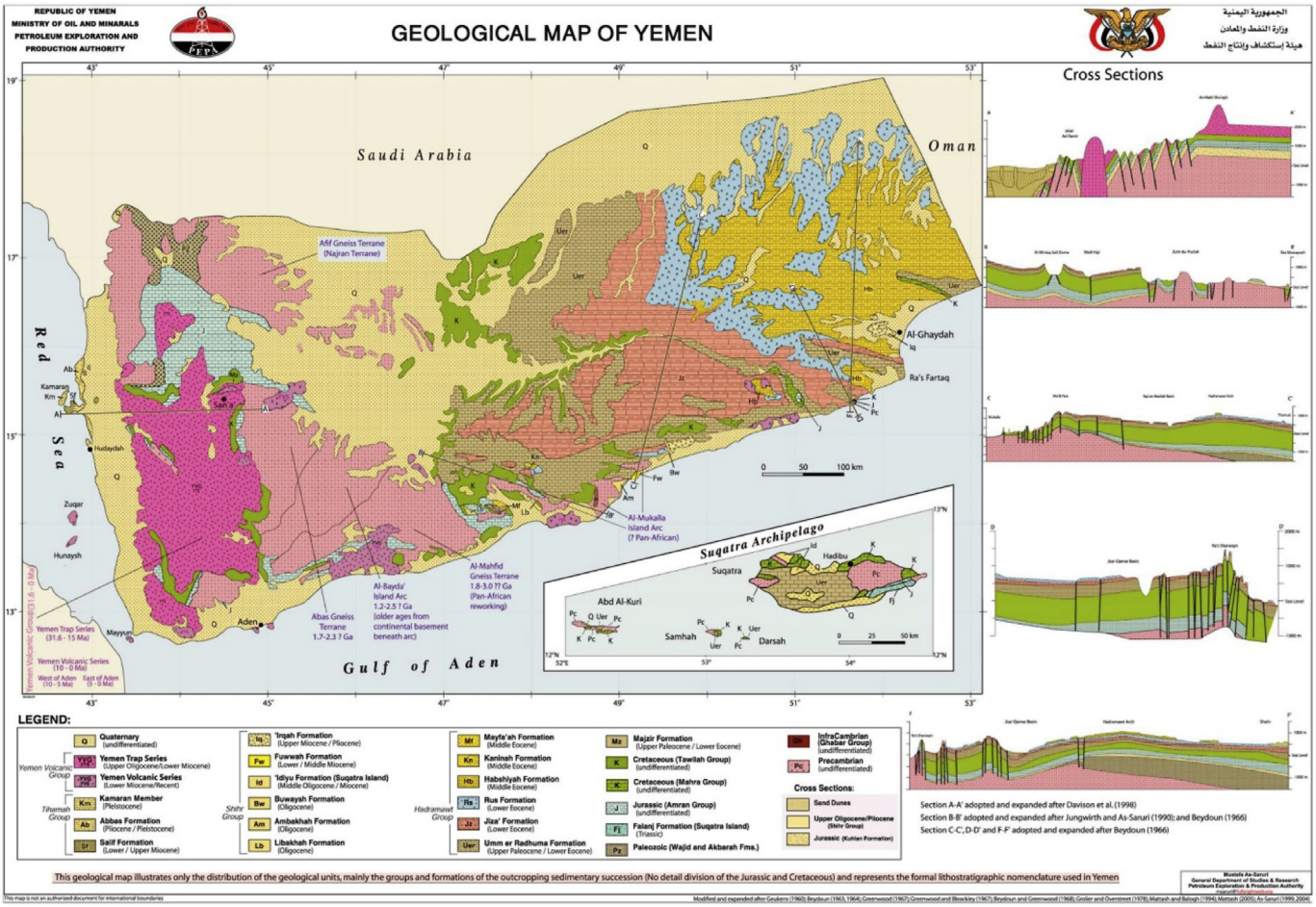

Figure 3. Geological map of Yemen. Reproduced from ref. [29] with the permission of Elsevier publishing, 2021.

was followed by aftershocks that lasted until the middle of March 1983. The one that was widely felt occurred on December 30, 1982, with a magnitude of $M = 5.3$. The Jahran Basin, the small Dhawran Basin (southwest Ma'ber), and the surrounding area are all affected. The Jahran Basin and surrounding areas are classified as highlands due to their depressed plains that span 90 km long and 40 km wide and are located between latitudes 14.5N and 14.10N. The entire region is composed of broad plains (trough, smaller valleys with a complex of mountains, hills plateaus and lava flows). The region is distinguished by a variety of rock types and sedimentary accumulations with varying thicknesses. This condition resulted in various ground accelerations, which caused varying degrees of destruction in the region, including the spread of cracks and faults in rocks (the most famous being the 5 km ground crack in Jahran Basin), the failure of water wells, differences in underground water level, the disappearance of some water springs, sporadic mountain failures, and various effects on structures. In accordance with the USGS [31], unverified reports showed that the 1982 Dhamar earthquake killed 2,800 people, injured 1,500, displaced 700,000 people, and destroyed or severely damaged approximately 300 villages in Yemen. Maximum intensity VIII in the Dawran–Risabah area was felt throughout Yemen and in Saudi Arabia's Najran region (Figure 5). Landslides and extensional earth fractures running north–northwest in zones up to 15 km length occurred in the epicentral region. This hypocenter is the first instrumentally discovered in the Dhamar area. Figure 5 depicts the intensity data obtained during the Dhamar earthquake on Dec 13, 1982, in accordance with the USGS [31].

3.3. Recent seismic activity - for the period 1986–2021

The Yemen national seismic network recorded seismic activity during this time period. In accordance with the NSOC [34] and USGS (PDE/EDR) [31] Annual Seismic Bulletins, the seismic records for this period show low to moderate seismicity with shallow earthquakes (depth 10–30 km) and $M \geq 4.0$ in and around Yemen up to August 2021. The Al-Udayn Earthquake (November 22, 1991) and the Haidan Earthquake (January 9, 1993) earthquakes were the most destructive large earthquakes that occurred during this time period. The seismotectonic map of Yemen is depicted in Figure 2 (epicentral distribution up to August 2021). On November 22, 1991, an earthquake with a magnitude of $M =$ 4.7 struck the Al-Udayn area, which is 40 km southwest of Ibb Governorate. This event was followed by aftershocks and swarms that lasted several months. The epicenter was near the villages of Bait Al-Shiber and Jabal Bahri, along the Wadi-Masirib. In accordance with the swarm epicentral distribution from USGS, the focal depth ranges from 1 km to 7 km. This earthquake killed 11 people and destroyed numerous buildings. On January 9, 1993, at 9:00 p.m., an earthquake with magnitude $M = 4.5$ struck the Haidan area, which is 45 km southwest of Sa'dah Governorate. It was recorded by a portable seismic station in the Al- Udayn area. This event was followed by aftershocks that lasted for two months, with the majority of them occurring in Wadi-Haidan, which is a major fault in the area. Many buildings were damaged by the earthquake, and some rocks collapsed. The seismotectonic map of Yemen for the period 1900–1994 is depicted in Figure 6 [34]. Many seismic activities have occurred in the

Table 2. Catalogue of historical earthquakes in Yemen [30].

Year A.D	Date	Description	Approximate Location
742	-	Many villages overwhelmed by collapsing mountains	Between Shabwah and Ma'rib
827	-	Destroyed houses, villages and caused many deaths	Aden and Sana'a
1072	-	Destroyed houses, killing 50 people	Sana'a, Zabid, and Mukha
1154	Sep 11	Destroyed many villages, castles and dwellings. killing 300 people	Between Sana'a and Aden
1259	Nov 22	Slight shock, no damage	Sana'a
1259	Dec 10	Damage to many places in mountains west of town	Sana'a
1265	-	Shocks were felt	Sana'a
1349	November	Caused panic, no apparent damage.	Zabid
1359	-	Shocks continued intermittently form midday to early evening. Many houses were destroyed	Zabid, Sana'a, and Aden
1387	September	Destroyed many houses without loss of life. Followed by shocks that lasted several days.	Aden
1394	March to April	Sequence of about 40 shocks felt.	Mawza Region
1427	-	Main shock and numerous aftershocks. Many houses were destroyed, about 60 killed.	Zabid
1463	-	Series of shocks over 3 days, 50 houses destroyed, 10 killed.	Zabid
1502–1503	-	Series of shocks. Panic but no damage.	Zabid
1504	-	Felt in Zabid	Near Zayla Somalia
1509	-	Series of large and small shocks	Mawza-Zabid
1613	-	Made ground swell in waves, possibly offshore epicenter.	Aden
1644	Sep 22	Strong tremor caused rock fall. May have been a landslide rather than an earthquake.	Al-Ashshah East of Sa'dah
1647	-	Shocks felt	Sana'a
1667	March	Damaged houses, felt throughout most of Yemen,	Sana'a
1674	August	About 30 shocks, culminating in a major shock in 1675	Dhawran
1675	-	Major shock, split many houses and caused rock falls from jabal Dawran. Felt in Sana'a	Dhawran
1788	End of Nov	Large shock affected Bayt Qasr and Bayt Hindi. Houses and buildings destroyed	Hudaydah
1789	July	Felt from Mukha to Abu Arish	
1859	Early January	Series of shocks possibly from an offshore event.	Aden and Mukha
1873	-	Landslide from a mountain near Bayt al-Nash	Al-Haymah West Sana'a
1878	-	Sequence of earthquakes and tremors lasted for three months, destroyed many houses	Dhamar-Yarim
1895	August 2	Series of shocks. Damage unknown	Mukha- Taiz

last decade, including but not limited to the following incidents: M 4.4–18 km NNE of Jawf al Maqbabah, 2015-03-18 01:09:18 am 13.975°N 45.927°E10.0 km depth, M 4.9–28 km WNW of Al Bayda, 2016-05-24 17:43:28 14.089°N 45.329°E10.0 km depth, M 4.7–140 km SW of Mukalla, 2018-10-23 22:26:58 13.652°N 48.197°E10.0 km depth, and M 5.2–147 km SSE of Mukalla, 2021-08-10 15:25:12 13.306°N 49.625°E10.0 km depth.

4. Input for PSHA in Yemen

Input seismic parameters should be evaluated to create a seismic hazard map and estimate ground motions caused by future earthquakes. PSHA has gained widespread acceptance and is regarded as seismology's most significant contribution to earthquake hazard assessment [35, 36, 37]. The following input parameters are required for performing a PSHA using the Cornell CA (1968) [38], McGuire RK (1976) [39], and Reiter L (1990) [40] approach.

1. Earthquake recurrence rates and potential earthquake magnitudes for Yemen are researched by using tectonic knowledge, an earthquake catalog, and historical earthquake information.
2. Seismic source regionalization (seismic zones) is a research element that entails identifying and regionalizing seismic sources. A seismic source is defined as an area in the Earth's crust where future earthquake recurrence is expected to be homogenous. Seismic regionalization is described as the separation of an earthquake activity zone into zones with comparable seismic activity on the basis of geology (geomorphic and stratigraphic) and historical criteria. Seismotectonic maps are used for the delineation of seismic sources and associated regionalization.
3. Data treatment. Having complete and ready-to-use data is rarely possible. This condition is particularly true in regions that are deficient in historical records and a seismographic network, which is also the case in Yemen. The data treatment process typically entails the following major steps.
   a) Clean up the earthquakes catalogues (removing of repetitive information & unifying magnitudes)

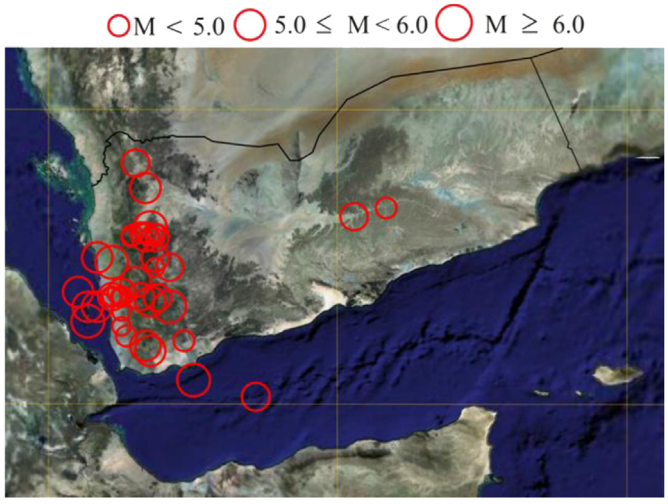

Figure 4. Seismotectonic map of Yemen for the period 742–1899. Reproduced from ref. [34] National Seismological Observatory Center (NSOC), Dhamar, Yemen.

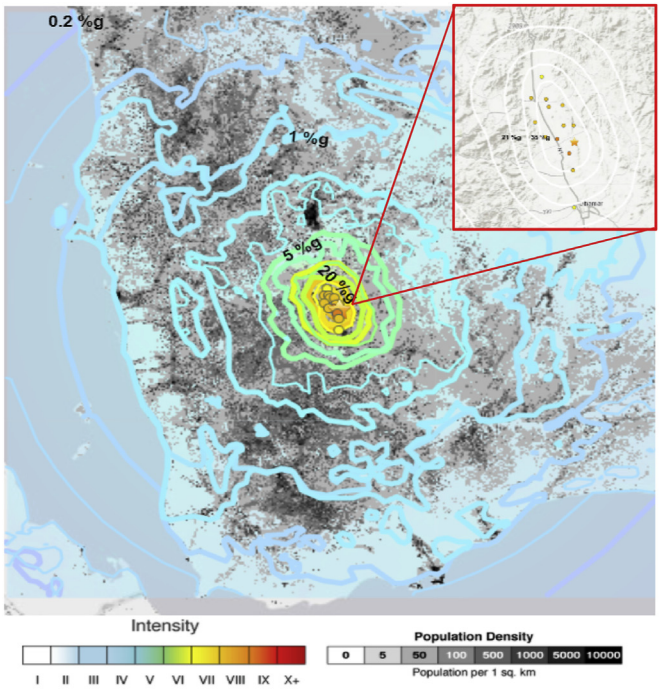

(a) PGA, intensity, and population density Map USGS Shake Map: Dhamar earthquake Dec 13, 1982 UTC M6.3 N14.70 E44.38 Depth: 5.0 km.

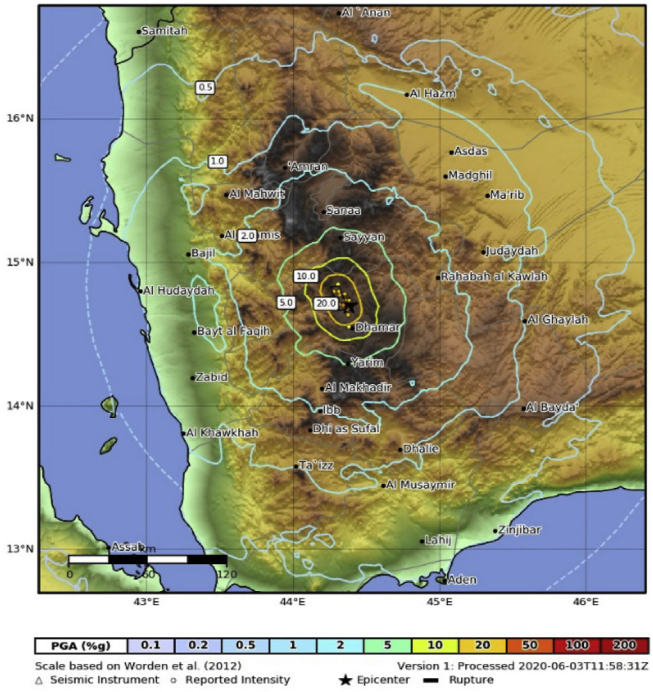

(b) PGA Map USGS Shake Map: Dhamar earthquake Dec 13, 1982 UTC M6.3 N14.70 E44.38 Depth: 5.0 km.

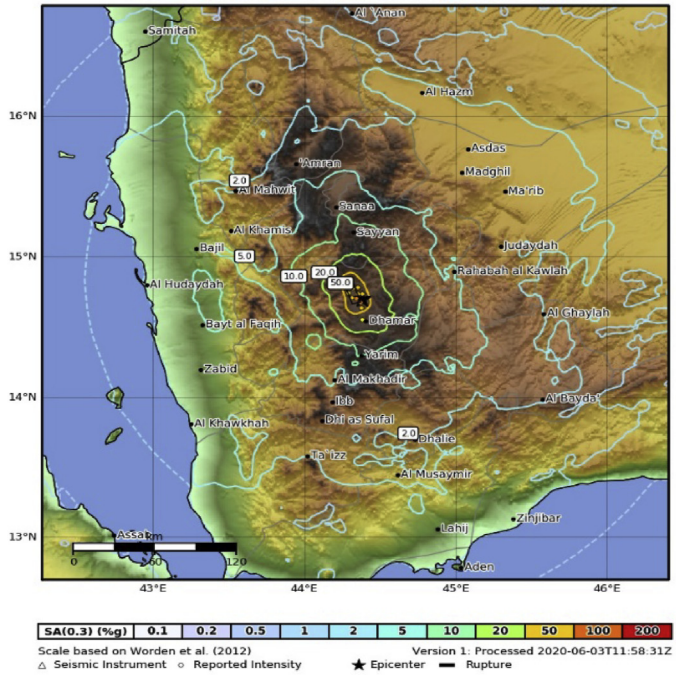

(c) 0.3 Second Peak Spectral Acceleration Map USGS ShakeMap: Dhamar earthquake Dec 13, 1982 09:12:48 UTC M6.3 N14.70 E44.38 Depth: 5.0 km.

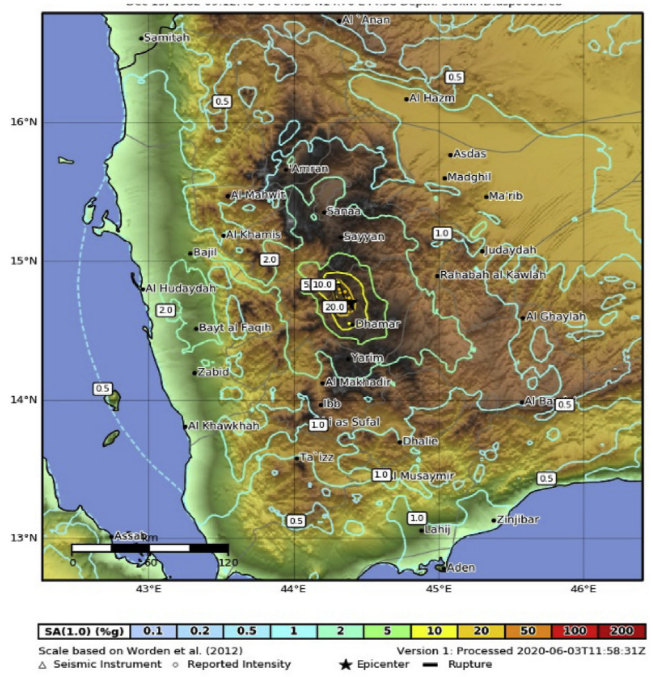

(d) 1.0 Second Peak Spectral Acceleration Map USGS ShakeMap: Dhamar earthquake Dec 13, 1982 09:12:48 UTC M6.3 N14.70 E44.38 Depth: 5.0 km.

Figure 5. The intensity data obtained during the Dhamar earthquake on Dec 13, 1982. Reproduced from ref. [31] USGS.

b) Identification and elimination of clusters (secondary events that come in the wake of major events).
c) Evaluation and distribution of missing magnitudes
d) Incompleteness analysis of the earthquake catalogue.

4. An earthquake recurrence relationship for each source describes the seismicity recurrence characteristics of the seismic sources. The size of the largest earthquake that will be utilized as the upper cutoff magnitude in the linear recurrence relationship is calculated for each source. This variable is one of the most divisive and crucial to consider when attempting to represent source seismicity.
5. An attenuation of ground motion amplitudes is predicted by using a predictive ground motion model, which predicts the decrease in

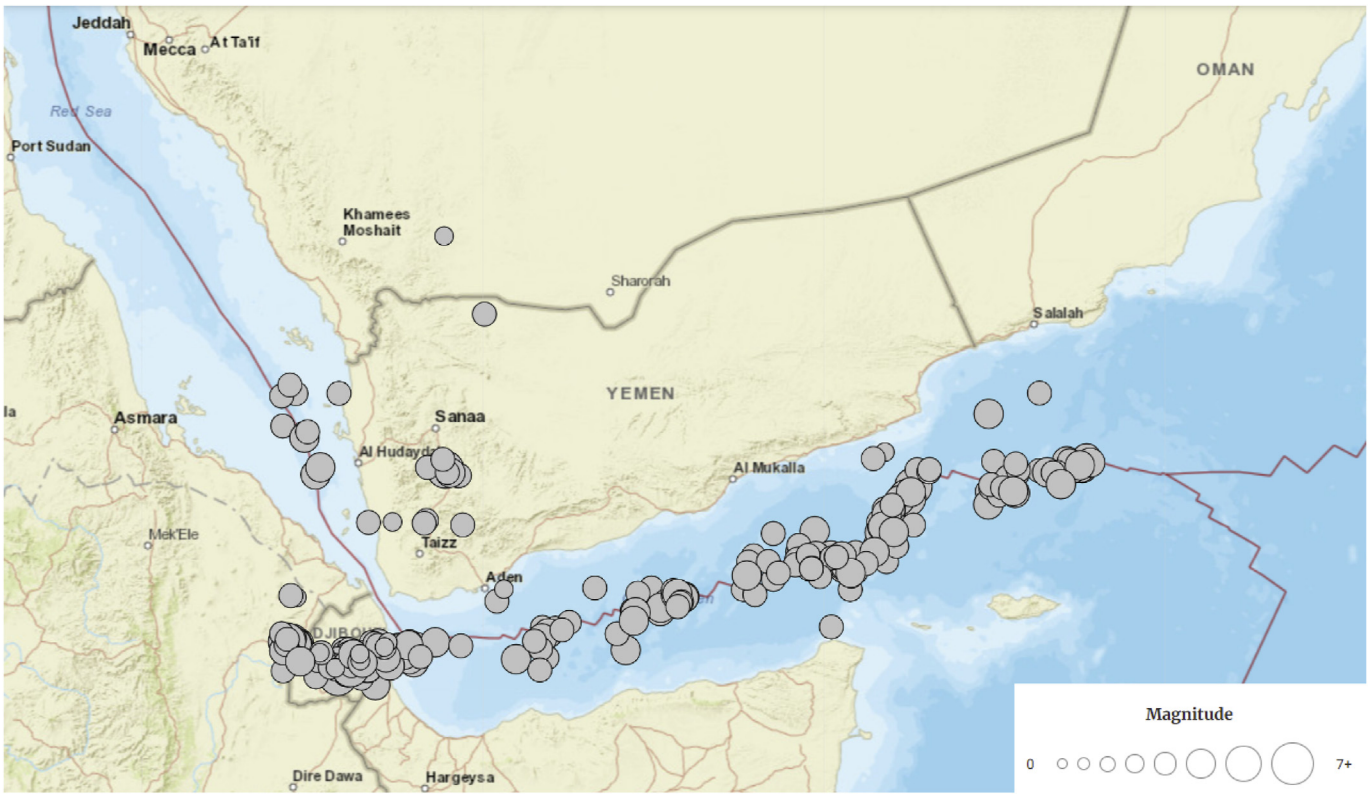

Figure 6. Seismotectonic map of Yemen for the period 1900–1994. Reproduced from ref. [31] USGS.

amplitude as a function of distance and magnitude. The methodology used to obtain these Yemen input parameters is explained.

4.1. Earthquake catalogs and tectonic information

4.1.1. Nonduplication of seismic data

The statistical characterization method for seismogenic source zones in Yemen utilized three different sets of seismic data in different observation periods. The first is labeled as historical data (112–1964 AD), and the second is labeled as instrumental data for the sake of discussion (1965–1985 AD). The first two sets are typical samples of the source catalogs used to generate the seismic data, and the third set contains more current data (1986–2021AD). The source catalogs from which the utilized seismic data are taken are the Ambraseys (1988) [18] from 112–1964 AD, USGS (PDE/EDR) from 1965–2021, ISC from 1965–2021, EMSC from 1990–2021, and NSOC, Dhamar, Yemen from 2000–2015. Seismic data from these numerous seismic bulletins were combined and collated to provide the primary database for delineating and identifying the various seismogenic source zones in Yemen and performing statistical analysis. Seismotectonic correlation of activity in each source region was performed by using the gathered seismic data. Limiting and differentiating methods for the space-time distribution of data events were used to minimize duplication in the intervening years of seismic data. When two or more data points have a difference in origin time of less than 25 s in a 200-km radius, they are considered to be a single event. For repeated occurrences, the USGS data are prioritized in the selection process.

4.1.2. Identification and elimination of clusters

The phenomenon of main shocks being followed by a number of aftershocks is well-known in earthquake mechanics (clusters). Merz demonstrated in 1973 [41] that aftershocks have a small contribution to seismic hazard estimates and that considering only main shocks is sufficient for engineering purposes. The presence of these aftershocks contradicts the Poison process' assumption of memorylessness, which is commonly used to forecast future earthquakes. Clusters were identified and eliminated in this study by using Gardner and Knopoff's windows algorithm (1974) [42]. The algorithm begins by generating time and space windows around the main shocks, which grow in size with the increase in the magnitude of the main shock. Small and moderate earthquakes, as opposed to the main shock, were identified and removed from the space and time windows. Table 3 shows the discrete time and space windows used in Gardner and Knopoff 1974 [42]. These windows are used to create a continuous model for the two windows by using regression analysis. Linear regression analysis is used for the distance window, and nonlinear regression analysis is used for the time window. The regression analysis is depicted in Figures 7 and 8. The developed earthquake magnitude equations are as follows:

$$\text{Time (days)} = 0.0123\ \text{Mag}^{5.903}, \quad (1)$$

$$\text{Distance (km)} = 11.786\ \text{Mag} - 17.071. \quad (2)$$

Table 4 presents the calculated time and space windows for various levels of earthquake magnitudes. The algorithm for identification aftershocks in an area source can be summarized in the following steps.

Table 3. Windows algorithm for aftershocks according to Gardner & Knopoff, 1974 [42].

Magnitude	Distanced (km)	Time (days)
3.5	26	22
4	30	42
4.5	35	83
5	40	155
5.5	47	290
6	54	510
6.5	61	790

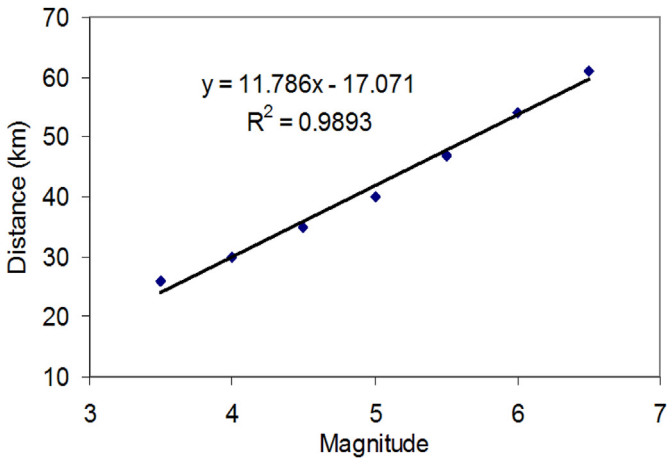

Figure 7. Distance windows for aftershocks.

1. Sort all events in the area source in an ascending order in accordance with time.
2. Select the first event in the list.
3. Calculate the time and distance windows in days and km, respectively, by using the developed Eqs. (1) and (2).
4. Open the time window and identify all events within this window.
5. Compute the distance from the selected event to those events.
6. Check all smaller and equal events within the distance window. These events are the aftershocks of the selected event.
7. For those events that are outside the time or distance windows, repeat steps 2 to 6 to identify their aftershocks.
8. Eliminate all aftershocks from the list.

4.1.3. Incompleteness analysis

Incomplete seismic data are unavoidable because many variables affect the processing and compilation of the necessary data. In seismic observation, the paucity and inadequacy of physical elements and the absence, inadequacy or poor detection capacity of sensing equipment are all examples of these influencing variables. Incomplete earthquake catalogs introduce bias in earthquake recurrence model parameter estimations when analyzed over the full scope of recorded history. Studies on incompleteness analysis for earthquake catalogues have been performed extensively, and several methods have been developed. In previous studies, incompleteness is commonly addressed by utilizing earthquake detection and reporting probabilities. These probabilities and their corresponding relative ratios are completely subjective.

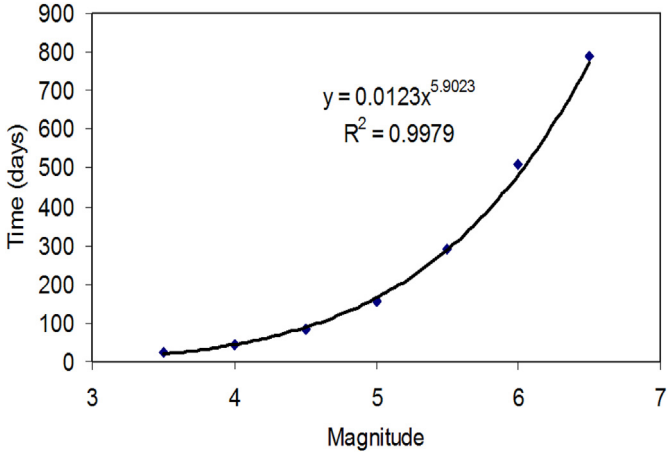

Figure 8. Time windows for aftershocks in terms of magnitude.

Table 4. Calculated time and distance windows from epicenter.

Magnitude	Distanced (km)	Time (days)
3.6	25.4	23.6
3.7	26.5	27.8
3.8	27.7	32.5
3.9	28.9	37.9
4	30.1	44.0
4.1	31.3	50.9
4.2	32.4	58.7
4.3	33.6	67.4
4.4	34.8	77.2
4.5	36.0	88.2
4.6	37.1	100.4
4.7	38.3	114.0
4.8	39.5	129.1
4.9	40.7	145.8
5	41.9	164.2
5.1	43.0	184.6
5.2	44.2	207.0
5.3	45.4	231.6
5.4	46.6	258.7
5.5	47.8	288.2
5.6	48.9	320.6
5.7	50.1	355.9
5.8	51.3	394.4
5.9	52.5	436.2
6	53.6	481.7

Earthquake magnitudes are classified into seven categories. The category interval is 0.4. The annual frequency of each category is calculated in the three time periods of records: the historical (up to 1964), the intermediate records (between 1965 and 1985), and the recent records (between 1986 and 2021). Correction factors based on the estimated probabilities of detection are used to modify these frequencies. These factors are listed in Table 5.

4.1.4. Missing magnitudes

Missing magnitudes were ignored because the magnitude interval defining the missing magnitude is extremely wide, approximately 1.5–2 magnitude units in the historical and early portions of the instrumental period, as determined from Ambraseys' research (1988) [18]. Comparing the impact of the distribution and inclusion of these magnitudes to that of the existence of clustering in the data are possible because many uncertainties are found in the suitable magnitude values. The missing magnitudes for the recent seismicity period are expected to be less than magnitude 4.0 due to appropriate seismic instrumentation, and these missing magnitudes are ignored in the data because they were less than the minimum magnitude threshold value of 4.0.

Table 5. Incompleteness correction factors.

Magnitude	Historical Period	Instrumented Period	Recent Period
4.4	3	1.5	1
4.8	3	1.5	1
5.2	2	1	1
5.6	2	1	1
6	1.5	1	1
6.4	1.5	1	1
6.8	1.5	1	1
7.2	1	1	1

4.2. Seismotectonic source models

On the basis of previously published studies (e.g., Ambraseys [18], Al-Haddad et al. [7], Al-Sinawi et al. [30], Al-Amri et al. [23], and Al-Amri [43]) focusing on the Arabian Peninsula, of which Yemen is a part, the characterization of Yemen's seismogenic source zones is divided into two parts. Brief explanations are provided for each source zone's possible connection to the tectonic and seismicity models of the regions inside each source zone. The other part is a logic tree diagram, which depicts the physical and seismic factors utilized in seismotectonic correlation. Only the logic tree for zones 3 and 7 is shown here as a model of the logic tree used in this study. The type of logic tree used is depicted in Figures 11 and 12 [23]. Seismicity and fractures were investigated by using two different methods in the research. A seismicity method uses a collection of seismic data from each source zone to estimate the magnitude–frequency connection and the linear slip and moment release rates. Frequency graphs were used to identify the particular seismicity characteristics for association with geological structures and possible earthquake source processes. The second method was used to investigate the tectonic structures included in each source zone by using current geological/tectonic maps to identify and associate them with different types of earthquake source mechanisms and the source area's seismicity. Combining the two methods led in the development of a preliminary framework for a seismotectonic model for each seismogenic source zone [23].

The results indicated that the tectonic model has only two possible sources, namely, the area and fault sources. Area sources include seismic events that are indirectly linked with the known existence of fractures or are off-location abd abrupt or randomly dispersed ground dislocations within the source zones. The sources of these seismic events under the area source might be vertical and lateral structural discontinuities or they can be associated with some unusual behavior of geophysical phenomena and/or beneath-surface cracks. Under the fault source, transcurrent and normal faults and their variations, are identified. Earthquakes are caused by two processes. Extrusion and transcursion are the mechanics involved. Extrusion zones are volcanic hotspots with rapid heat movement. Seismic and other geophysical data identify ridges and their continental expansion due to rifting, spreading, and other extensional tectonic features [23].

4.2.1. Seismic source zones

Seismotectonic maps, epicenter clustering, and seismicity smoothing were used to define 11 seismic sources displaying seismicity characteristics for Yemen. Figure 9 and Table 1 depict the present authors' seismogenic source model for Yemen, which is based on the seismotectonic setting described above and previously published research for the Arabian Peninsula (e.g., Al-Amri et al. [23] and Al-Amri [43]) (Figure 10).

The majority of seismic zones in Yemen are connected with active tectonics along the Sheba Ridge (zone 1), East Sheba Ridge (zone 2), and Gulf of Aden (zone 3), in accordance with this model (Figures 2 and 9). Considering the region's main seismogenic zones as area zones is recommended due to the difficulty in accurately defining the locations and slip rates of hidden blind faults in Sheba Ridge and East Sheba Ridge [24]. Sheba Ridge is divided into two areas. Between the late Campanian and early Mastrichian eras, a split occurred between Seychelles and India. Around 64 Ma, this rifting culminated in the Deccan volcanic eruption, which resulted in the formation of a new oceanic spreading zone, the Carlsberg ridge [43]. To the northeast of the Carlsberg ridge lies another ridge, the East Sheba ridge, which links the Gulf of Aden's major depression. The Sheba ridge is bisected by the Alula-Fartak trench to the west and the Owen fracture zone to the east. The epicenter distribution in this zone shows a significant relationship between seismicity and topography. The primary line of epicenters follows the crest of the Carlsberg ridge, which bends north–northeast at 10.5N, 57.0E and maintains this orientation until it reaches 13N. It makes a steep bend to the northwest at this latitude. The line of epicenters follows the axis of the Sheba ridge to approximately 56.5E, the location of the seismic occurrences [23]. This zone has been active throughout history and continues to be at present. The largest earthquake ever recorded in history occurred on August 17, 1899, with a magnitude of 6.6. This occurrence is situated away from the main ridge axis. On December 5, 1981, the instrumental maximum magnitude is 5.6. Its location is close to the main ridge [28]. Recently in zone 3, on

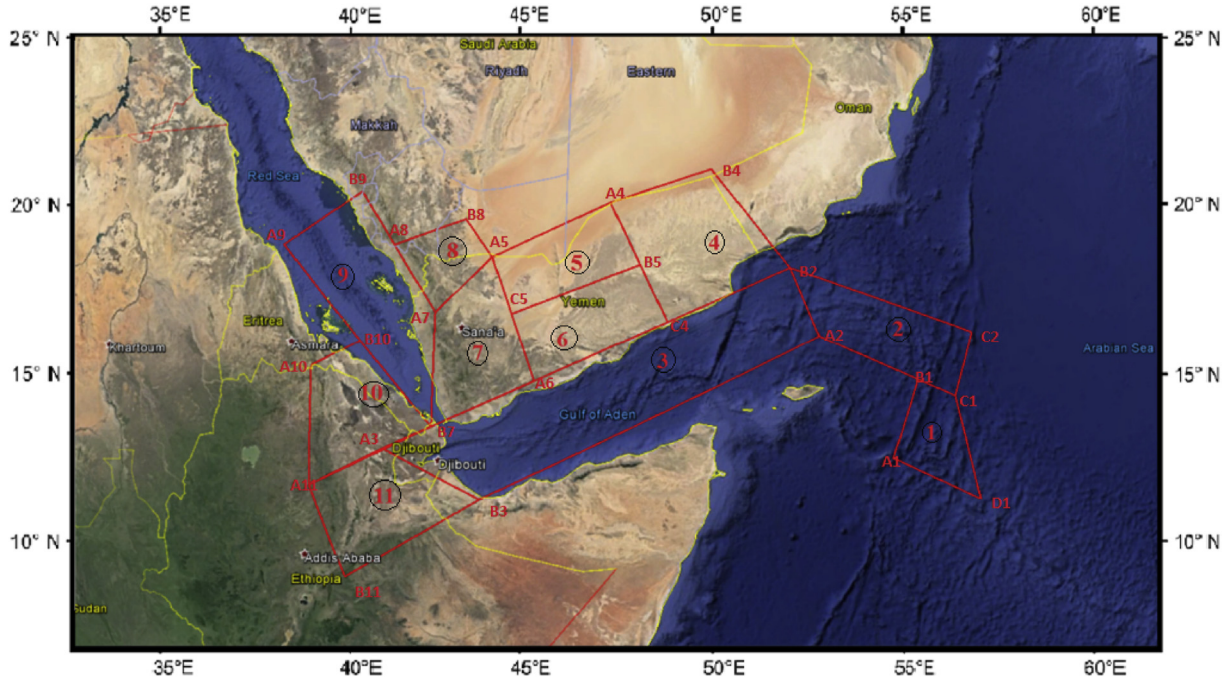

Figure 9. Delineated seismic sources in and around Yemen. Reproduced after modification from Google Maps, 2021.

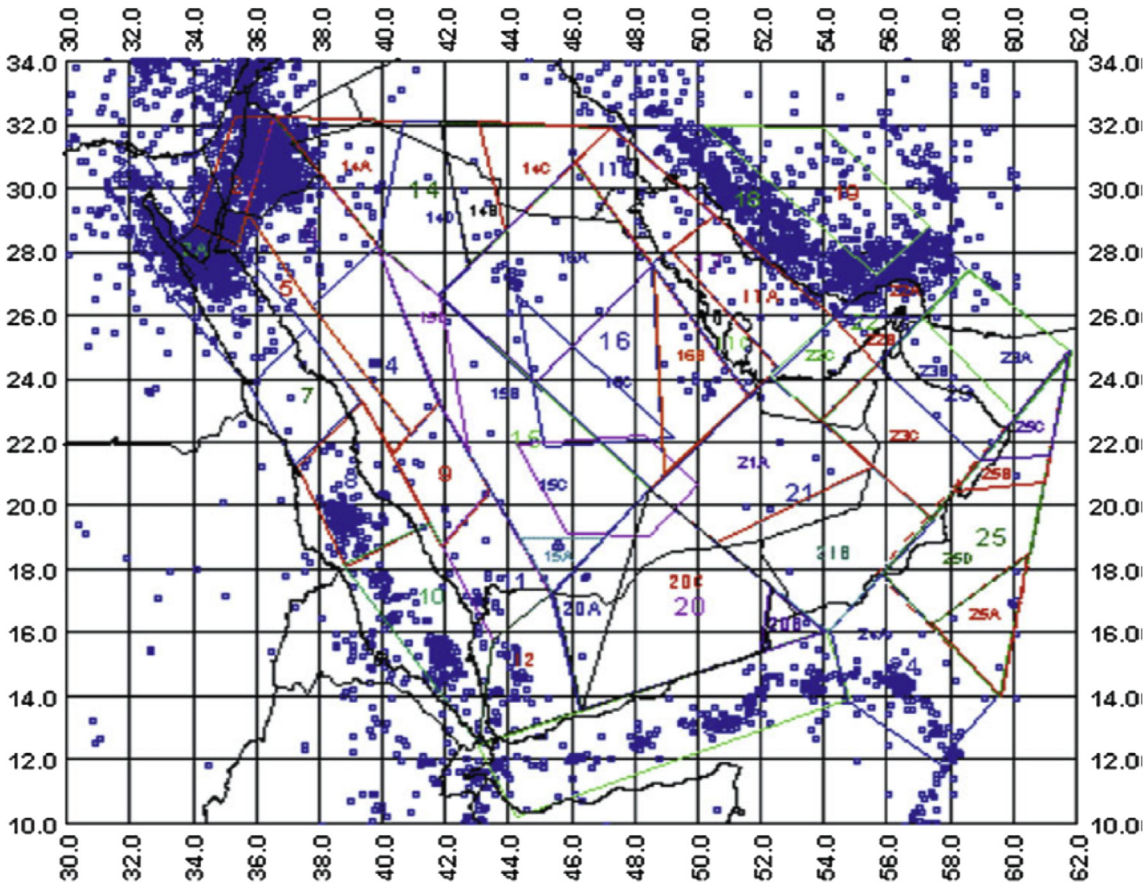

Figure 10. Seismicity and seismogenic source zones of the Arabian Peninsula and adjoining according to Al-Amri et al. 2004. Reproduced from ref. [23].

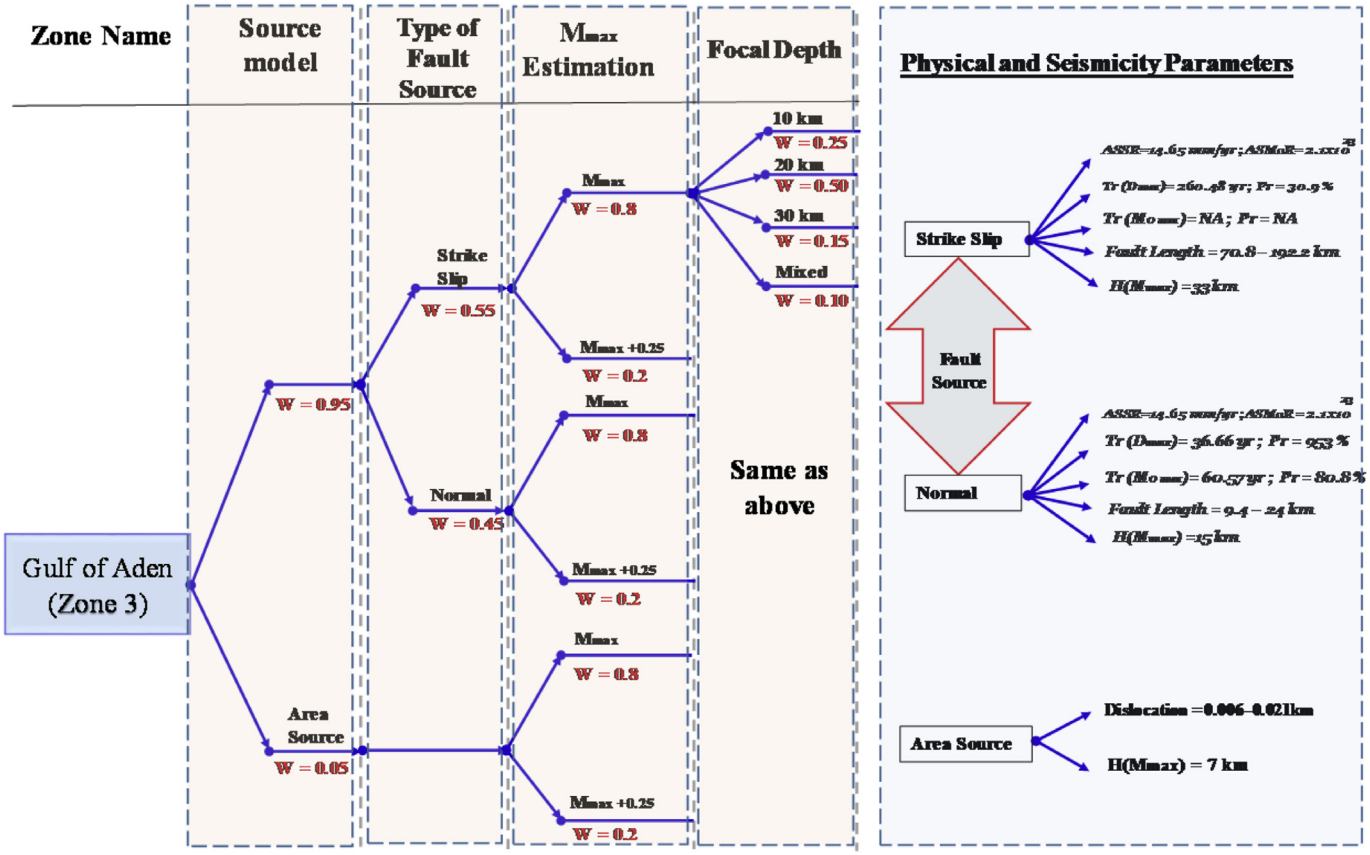

Figure 11. Logic tree diagram for Zone 3 (Gulf of Aden), modified after Al-Amri et al. [23].

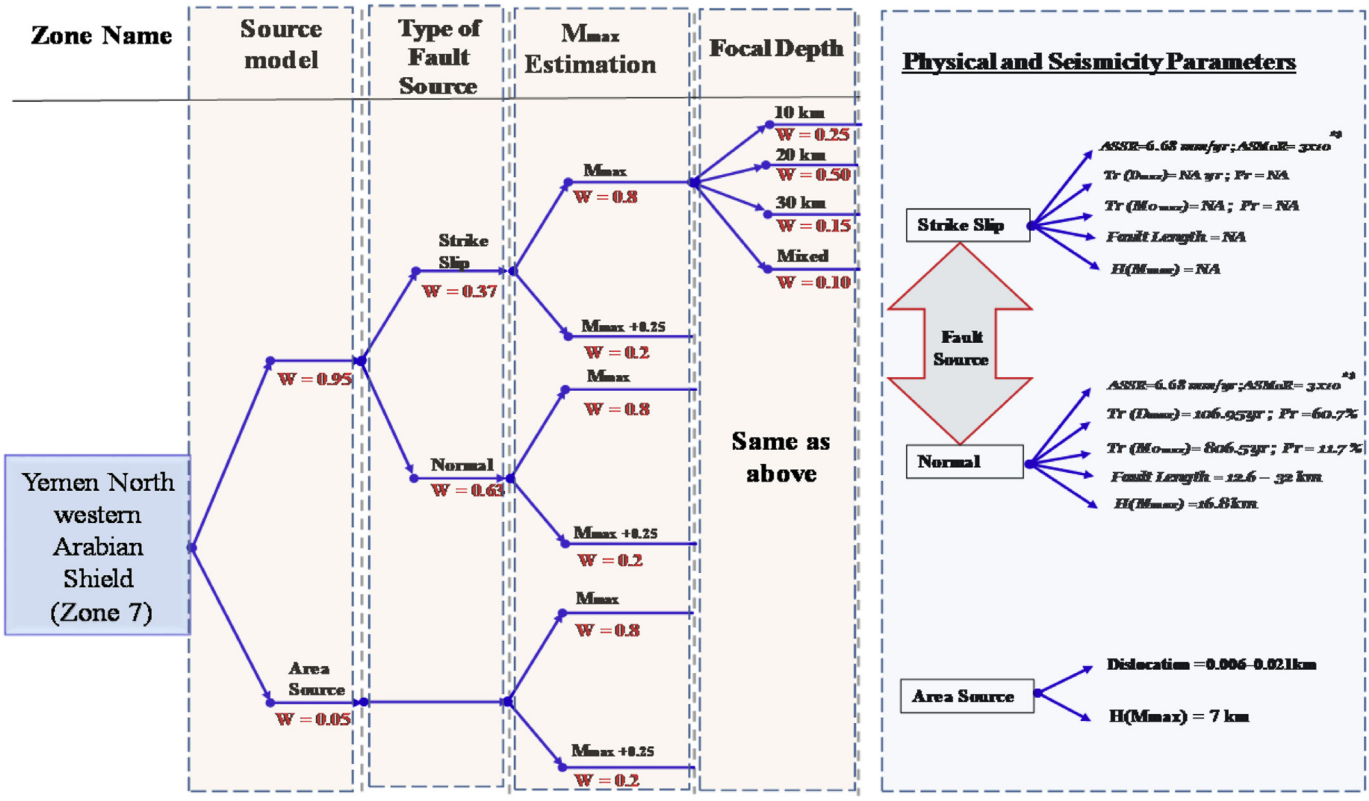

Figure 12. Logic tree diagram for Zone 7 (Yemen North western Arabian Shield), modified after Al-Amri et al. [23].

December 10, 2021, an earthquake with a magnitude of 5.2 was recorded (13.306°N 49.625°E).

The seismicity in the Gulf of Aden is modeled by using fault sources and area source zones (zone 3). The Gulf of Aden's seismicity level drops significantly as one travels away from the center axis, indicating that seismicity cannot be stable in space or time. This zone is determined to be seismically active throughout the whole monitoring period. The trend of the β-values throughout the two observation periods is upward, reaching its peak between 1965 and 1985. According to Al-Amri et al.'s [23] research, the logic tree diagram and recurrence relationship below illustrate the seismotectonic correlation for this source zone (3) (Figure 11). Each logic tree diagram uses the following symbolism (Al-Amri, A. M [43].: *ASSR* = average seismic slip rate in mm/year, *ASMoR* = average seismic moment release rate in dyne-cm/yr, *TrDmax* = approximate recurrence time in years of the maximum dislocation corresponding to M_{max}, H_{max} = crustal depth of structures corresponding to M_{max}, *Pr* = estimated probability of occurrence in 100 years of M_{max}.

Eastern Yemen is divided into three zones: The East Rub al Khali Arabian Shield (zone 4), the North Rub Al-Khali Arabian Shield (zone 5), and the Yemen Southern Arabian Shield (zone 6). Marib-Shabwa is a late Jurassic rift system in southern Yemen that runs west-–northwest–east–southeast. The system direction is compatible with the Najd trend, which most likely determined the orientation of the Jurassic rift. It is connected to a large network of basins that spans southern Arabia and the Horn of Africa. To the east, the system extends mostly to the Socotra island. During the Kimmeridgian-Tithon rifting era, the structural underpinning of the Marib-Shabwa Basin was created. The rift expands considerably in the Shabwa region, and major north–south (Hadramaut Trend) lineaments, such as the Shabwa arch and the Ayadin fault, are evident. This tendency may have been inherited from the suture of a Proterozoic arc terrane. The Marib-Shabwa basin is composed of a series of interconnected grabens and half-grabens. During and after the rift, the central Marib-Shabwa basin exercised considerable influence over sedimentation. During syn-rift periods, the deep half-grabens on the basin border and close to the Central High trapped clastics in their axes, depriving the central basinal regions of clastics. The direction of salt migration during postrift periods was determined by the block-faulted terrain, with salt creating linear ridges atop footwall highs. Therefore, postrift sedimentation was concentrated in a series of linear salt-withdrawal basins above syn-rift lows [23].

During the observation period, the Yemen North Western Arabian Shield (zone 7) has been seismically active. Seismicity is decreasing over time. The β-values in the first two stages of observation indicate a higher expectancy for large events. The highest observed magnitude in the historical period is a typical earthquake in the region. M_{max} for this period is estimated by using the truncated cumulative frequency distribution. The movement of the fault system in this area, such as the Sadah fault, is one of the most likely causes of the seismic activity. According to

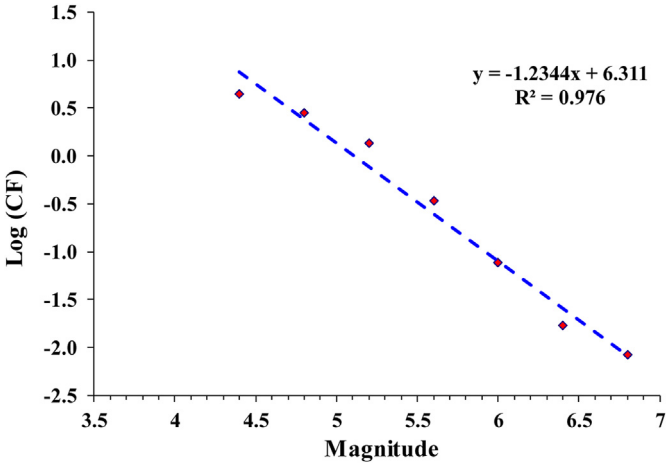

Figure 13. Recurrence relationship for source No. 2 (East Sheba Ridge).

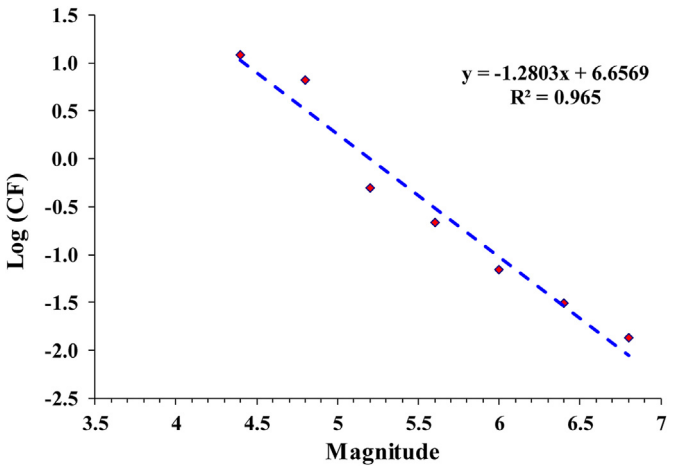

Figure 14. Recurrence relationship for source No. 3 (Gulf of Aden).

Al-Amri et al.'s [23] research, the logic tree diagram below depicts the seismotectonic correlation for this source zone (7) (Figure 12).

The Red Sea-Al Darb, African Southwestern Red Sea, and East African Rift zones have been seismically active throughout the observation period. The range of β-values indicates a moving-up trend with the progress of time. The recent activity has a higher expectancy for moderate events, and the two previous periods of observation have a lower expectancy for large events. The movements of the NE trending Ad-Darb transform fault and the basic intrusion of magmas in the Red Sea's axial rift, as indicated by the presence of deep holes and high heat flow, are two possible causes of seismic activity in this zone [28, 44].

4.3. Recurrence relations

4.3.1. Determination of β and λ values

Statistical regression analysis was used to find the line of best fit with the least squared error. The magnitude–frequency relationship for each individual source was expected to follow the Gutenberg and Richter (1944) [45] relationship defined by,

$$\log N(M) = a - b(M), \tag{3}$$

where N is the number of earthquakes of magnitude (M) or greater per unit time. The a value is the activity and defines the intercept of the above recurrence relationship [46] at M equal to zero. Figures 13 and 14 illustrate the recurrence relationships for a selection of sources (East Sheba Ridge and Gulf of Aden). The parameters for the recurrence relationships of all seismic sources in Yemen are shown in Table 6. In the remaining seismogenic zones, seismic activity was assumed to follow a doubly bounded exponential distribution (Cornell and Vanmarcke 1969 [46]). The following equation is used to approximate the truncated exponential recurrence relationship.

$$N(\geq M) = \alpha \frac{exp[-\beta(M - M_{min})] - exp[(M_{max} - M_{min})]}{1 - exp[-\beta(M_{max} - M_{min})]} \tag{4}$$

where $\alpha = N(Mmin)$, an arbitrary reference magnitude is M_{min}; M_{max} is an upper-bound magnitude, where N (M) is zero for any magnitude greater than M_{max}. The frequency of an earthquake (in a certain location) approaches zero if a maximum magnitude is established. We found the doubly bounded exponential distribution parameters in this research by using the maximum likelihood estimation method of Weichert (1980) [47].

4.3.2. Cutoff points

The regression analysis for evaluating recurrence parameters, which reflect the number of events above zero magnitude in a source and its seismic severity, is performed with the maximum magnitude as the upper cut-off. Earthquakes of magnitude less than 4 are disregarded in the analysis because they are of no engineering interest (especially in the design of seismic buildings). If a seismic zone is modeled as a combination of line source/s and area source/s, seismic activity in terms of the respected source zone is distributed among the different source models in this zone on the basis of contemplated ratios (Logic Tree), as shown in Figures 11 and 12.

The maximum magnitude (the upper cut-off), which is one of the most controversial and important variables of interest in representing source seismicity, is used as the upper cut-off magnitude in the linear recurrence relationship.

The current techniques for estimating the maximum earthquake include two approaches, neither of which is free of interpretive issues; the active fault approach and the historical earthquake approach [43]. For short return periods, the ground motions are dominated by the more frequent occurrence of low-to-moderate-magnitude events [43]. Thus, selecting upper-bound earthquakes is not a crucial factor in determining ground motion levels. Maximum magnitudes are determined by using various methods depending on the nature of the source zone (fault or area source) and the robustness of the available seismological database for each zone. Over the last several decades, regression relationships between earthquake magnitude and fault parameters have been developed (e.g., Slemmons et al. [48]; Bonilla et al. [49]; Wells and Coppersmith [50]; Hanks and Bakun [51]).

In this study, the cut-off magnitude is taken to be the observed maximum magnitude developed by the source plus 0.25, on the basis of a previous study by one of the authors (Al-Haddad, M., et al. [7]) and another study by Al-Amri et al. 2004 [23], which was applied in Yemen's

Table 6. Parameters of recurrence relationships for all area sources.

Zone No.	Zone Name	No. of events	α	β	λ	M_{min}	M_{max}	б M_{max}	M_{max} (obs)
1	Sheba Ridge	205	11.96	2.29	6.12	4.0	6.9	0.25	6.7
2	East Sheba Ridge	469	14.53	2.84	7.56	4.0	6.9	0.25	6.6
3	Gulf of Aden	775	15.3	2.94	10.55	4.0	6.9	0.25	6.6
4	East Rub al Khali Arabian Shield	5	-	-	-	4.0	5.2	0.25	4.9
5	North Rub Al-Khali Arabian Shield	-	-	-	-	4.0	-	0.25	-
6	Yemen Southern Arabian Shield	1	-	-	-	4.0	4.6	0.25	4.4
7	Yemen North western Arabian Shield	59	10.50	2.18	2.48	4.0	6.6	0.25	6.4
8	Yemen Southwestern Arabian Shield	8	9.73	2.43	0.38	4.0	5.9	0.25	5.7
9	Red Sea-Al Darb	147	15.22	3.21	3.01	4.0	6.6	0.25	6.3
10	African Southwestern Red Sea	264	13.72	2.64	7.88	4.0	6.8	0.25	6.5
11	East African Rift	52	6.04	1.33	1.17	4.0	6.6	0.25	6.4

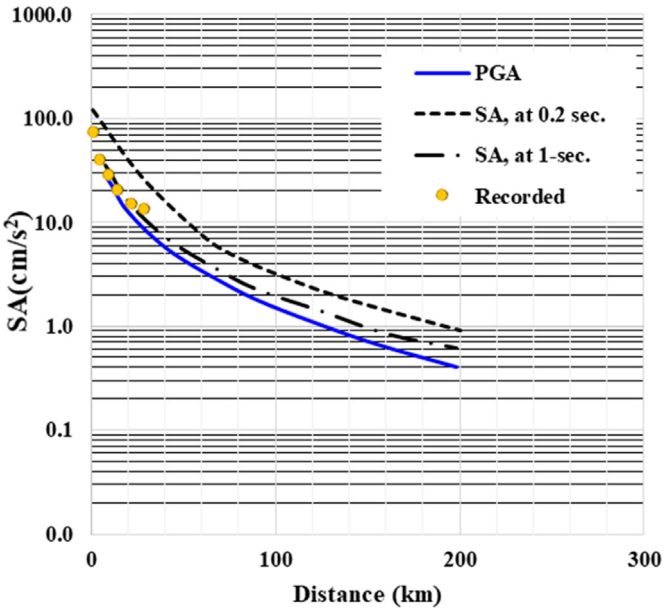

Figure 15. Ground motion attenuation relationship used in the study (Dhamar 1982 earthquake).

neighboring countries, particularly the Kingdom of Saudi Arabia. Table 6 includes these maximum magnitudes.

5. Attenuation models

An attenuation model provides estimation of ground motion intensity, such as PGA or SA, as a function of earthquake magnitude, site-to-source distance, and other essential seismic parameters. It is one of the most important components in seismic hazard analysis because the ground motion intensity can vary significantly depending on attenuation models to be used. Yemen and the Arabian Peninsula are still lacking earthquake ground motion records necessary for developing a reliable attenuation model for the region. Therefore, attenuation models developed from other regions of the world need to be adopted to best represent the geological and seismological attributes of the region. Different attenuation models result in different estimations, and determining which attenuation models are suitable for Yemen remains uncertain. This study attempts to use the most suitable attenuation relationships by comparing PGA estimates from several attenuation equations to a limited number of records that recently became available.

Ground motion scaling relationships have been used for different tectonic zones. This study used them to handle the epistemic uncertainty associated with the earthquake attenuation parameters for each tectonic province being unknown. Owing to no ground motion distance attenuation relationships developed specifically for Yemen, the models of the Saudi Building Code (AR-SBC) were used to model the ground motions from seismic sources and for the similarity of a mountain range in the border areas of Najran and Jizan called the Sarawat Mountains, which start in Asir in southern Saudi Arabia and extend to the Gulf of Aden in the south, running along the entire western coast of Yemen. This process shows that the terrain in the Arabian Peninsula has a similar character, and this model may be utilized and calibrated with the Saudi code in border regions with Yemen.

The majority of the efforts in developing the design Ground Motion of SBC were devoted to selecting an adequate ground motion attenuation relationship for use in the PSHA at each of the study sites. Several attenuation relationships were investigated and compared to ground motion acceleration data collected during the Gulf of Aqaba earthquake in 1995, Jizan earthquake 2014, Dhamar earthquake on Dec 13, 1982, and other earthquakes that occurred on the borders of Yemen and Saudi Arabia.

The most relevant attenuation relationship discovered is a refined version of Sadigh et al. (1997) [34] relationship and shows good agreement with the ground motion acceleration data recorded for Gulf of Aqaba earthquake in 1995 and Dhamar earthquake on Dec 13, 1982, as shown in Figure 15.

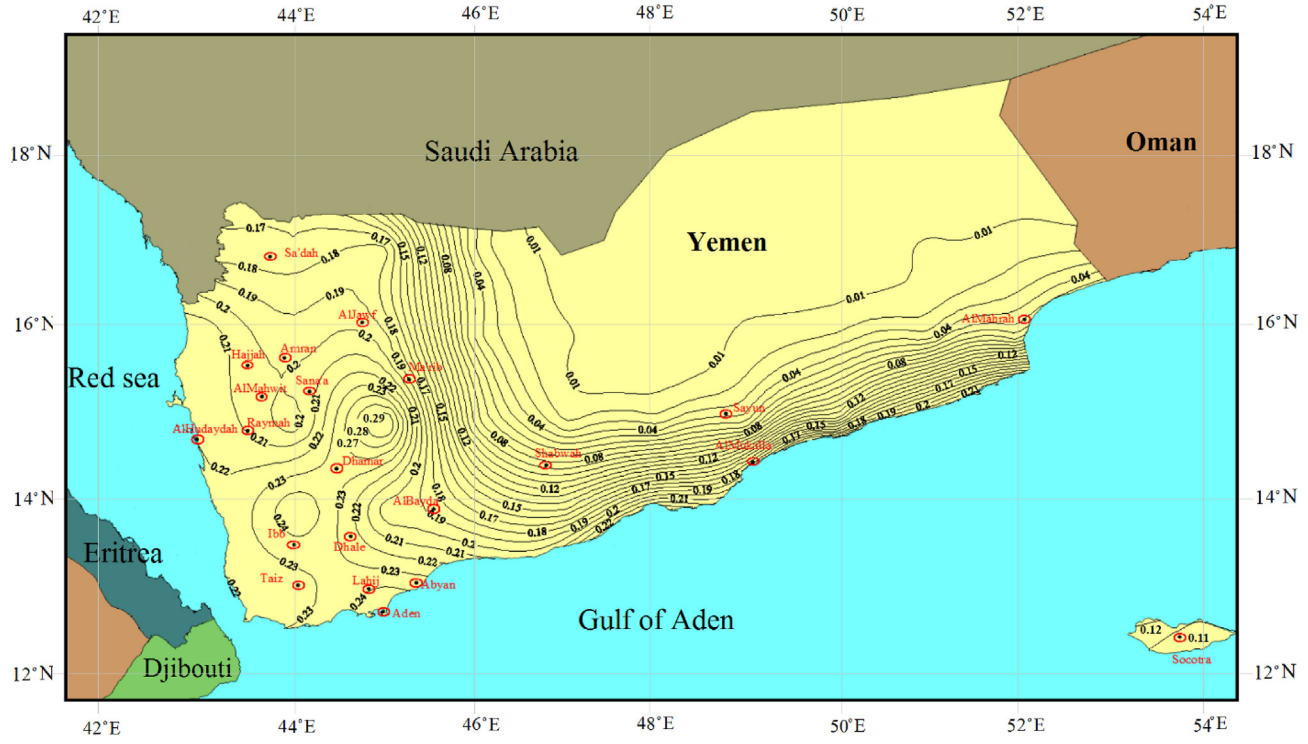

Figure 16. Mean peak ground acceleration (in %g) on rock sites with 10% probability of exceedance in 50 years (475 year return period) in Yemen Site Class B.

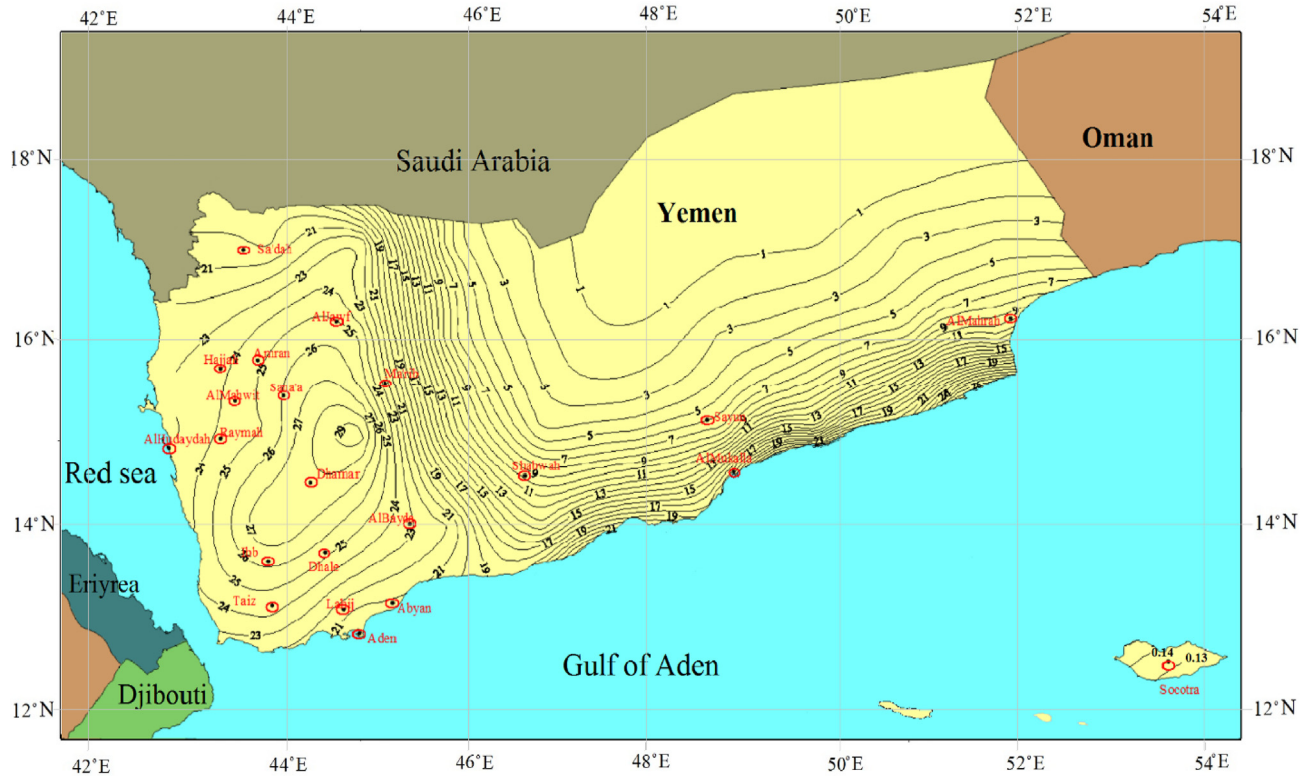

Figure 17. Maximum considered earthquake ground motion for Yemen of 1 s spectral response acceleration (S1 in %g) (5 percent of critical damping) Site Class B.

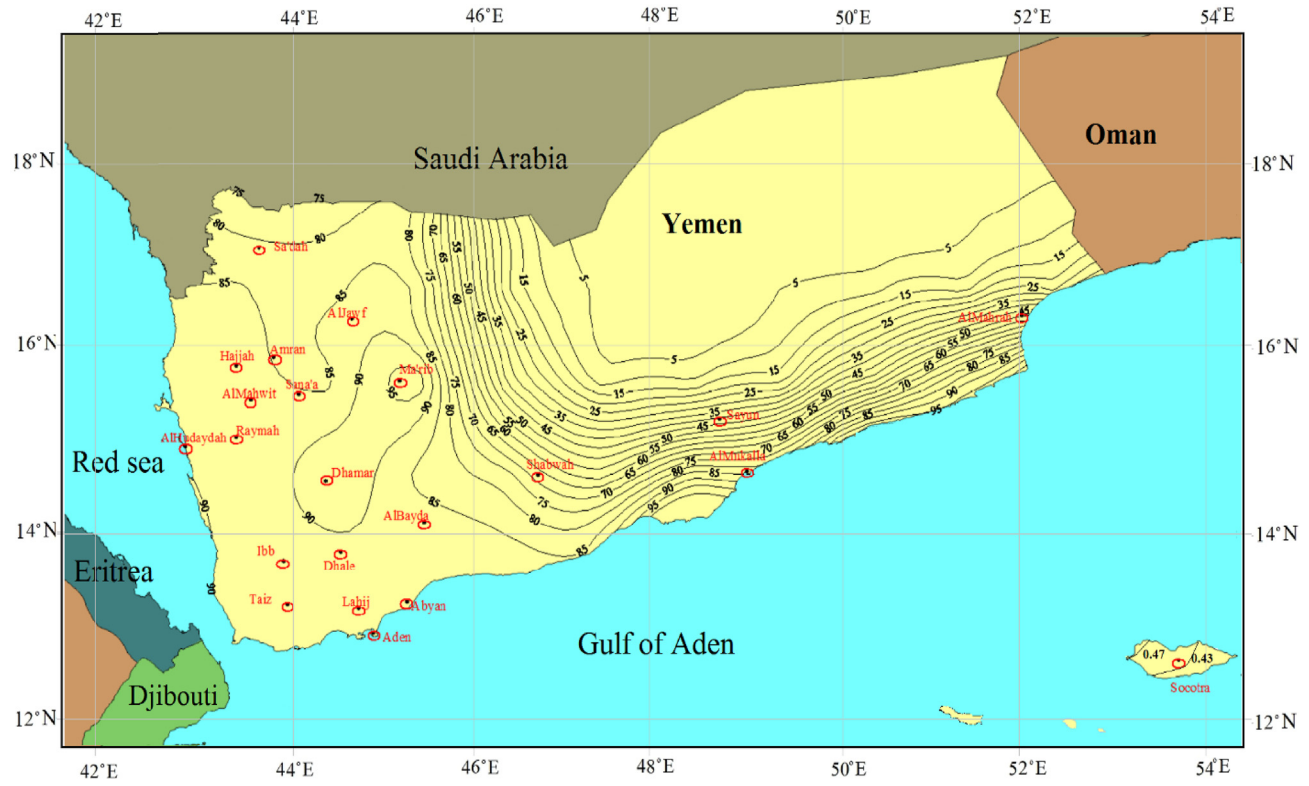

Figure 18. Maximum considered earthquake ground motion for Yemen of 0.2 s spectral response acceleration (Ss in %g) (5 percent of criti-cal damping) Site Class B.

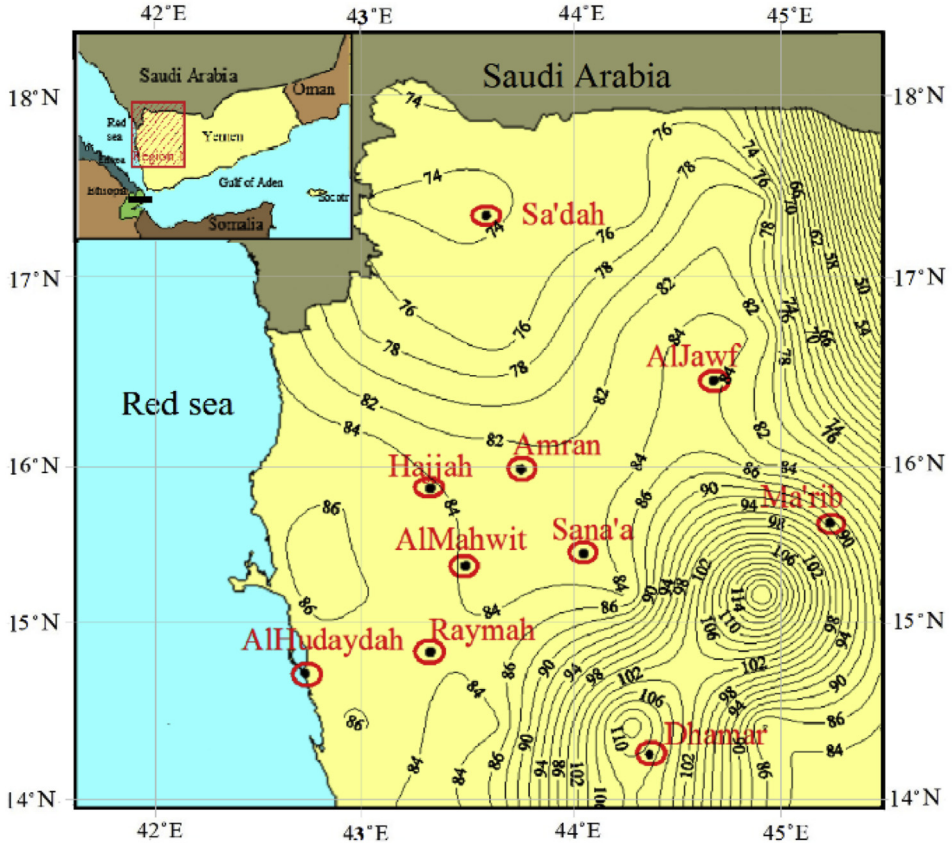

Figure 19. Maximum considered earthquake ground motion for northwestern region of Yemen: (a) 0.2 s spectral response acceleration (Ss in %g), (b) 1.0 s spectral response acceleration (S1 in %g) (5 percent of critical damping) Site Class B.

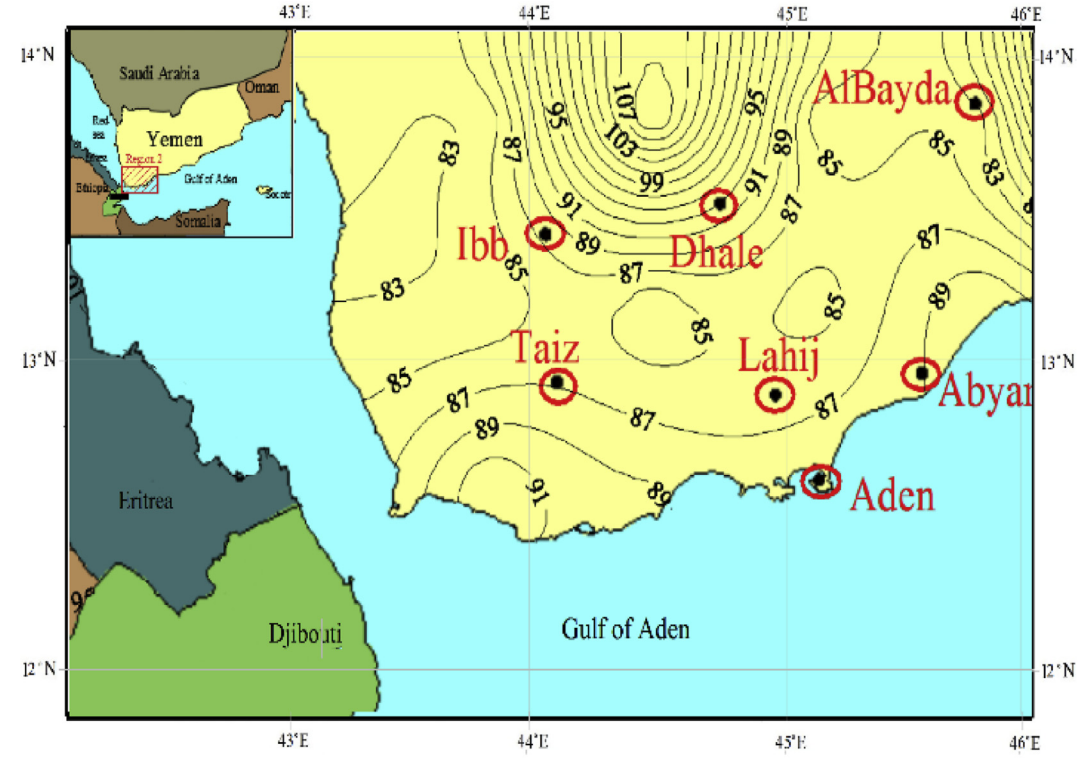

(a)

(b)

Figure 20. Maximum considered earthquake ground motion for southwestern region of Yemen: (a) 0.2 s spectral response acceleration (Ss in %g), (b) 1.0 s spectral response acceleration (S1 in %g) (5 percent of critical damping) Site Class B.

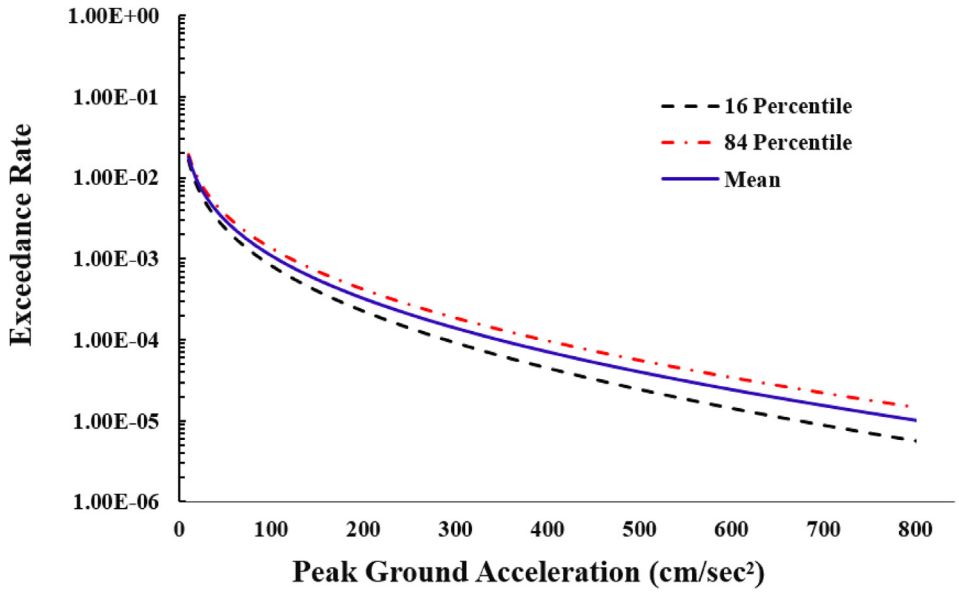

Figure 21. Seismic hazard curves for four Sanaa.

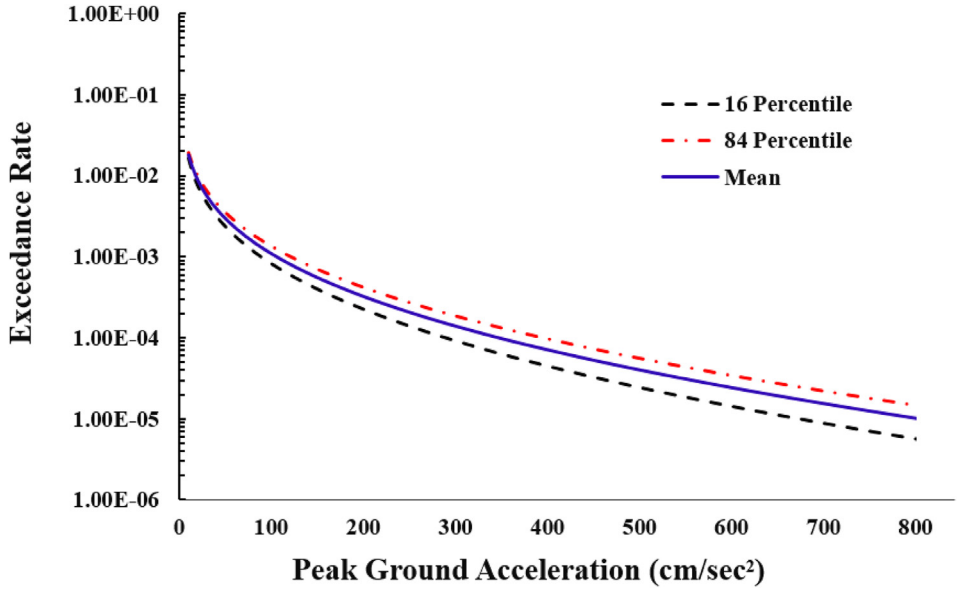

Figure 22. Seismic hazard curves for four Dhamar.

The attenuation relationship used for the analysis covers the relationships for the PGA and spectral SA for 14 periods of vibration (0.05 s–6 s) and magnitude (M) values from 4.4 to 8.0. It also includes the values for the site distance from the seismic sources, ranging from 5 km to 500 km.

6. Hazard calculations

In the current study, seismic hazard mapping is performed by using a probabilistic model (Figures 16, 17, 18, 19, and 20). Three Yemeni cities, Sana'a, Dhamar, and Aden, had their seismic hazard curves (exceedance rate as a function of peak ground acceleration ranging from 1 to 800 cm/s^2) drawn out (Figures 21, 22, and 23). Yemen-specific, general PSHA has occurred, and more precisely targeted unified hazard spectra for rock sites have been created in Sana'a, Dhamar, and Aden, which include hazard spectra with 72, 475, 975, and 2475 year return periods (Figures 24, 25, and 26). Knowing if certain ground motion levels will cause exceeding is essential. To evaluate the seismic hazard of the researched region, the researchers used the probabilistic method that applies the area and fault source model. The computer program, Crisis 2007 [2], was used to perform numerical calculations. For all Yemeni areas, the seismic hazard was estimated for various return periods of 475 and 2475 years (Figures 16, 17, 18, 19, and 20). The resulting seismic hazard maps were established in various PGA and SA (0.2, and 1 s). Seismic hazard values were calculated every 35 km across Yemen and its surrounding areas, for a total of 200 computation points.

In this study, the soil of Yemen was classified as B soil (site class B) conditions, with a return period of 475 years for PGA and 2475 years for S_s and S_1 (Figures 16, 17, 18, 19, and 20). This classification

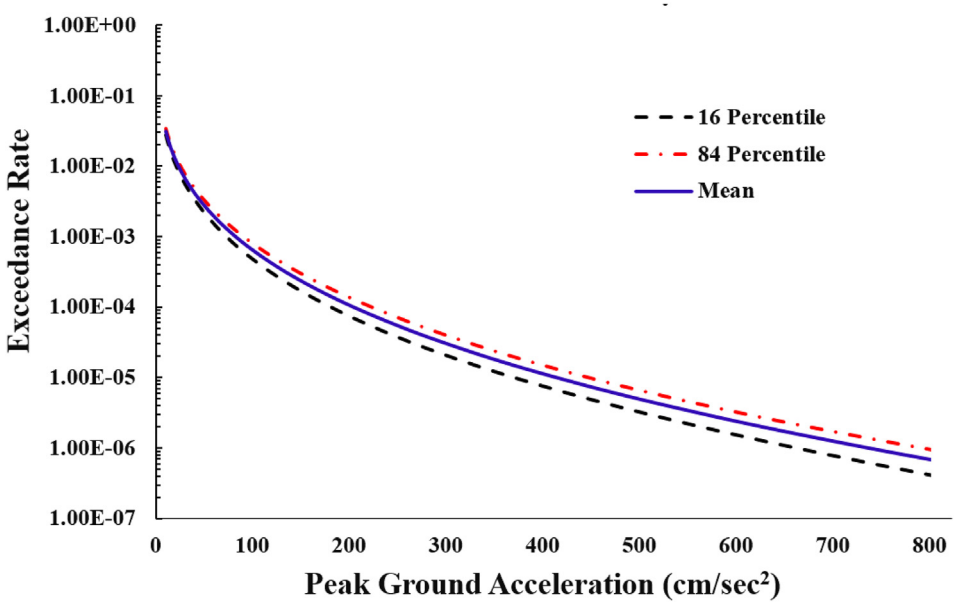

Figure 23. Seismic hazard curves for four Aden.

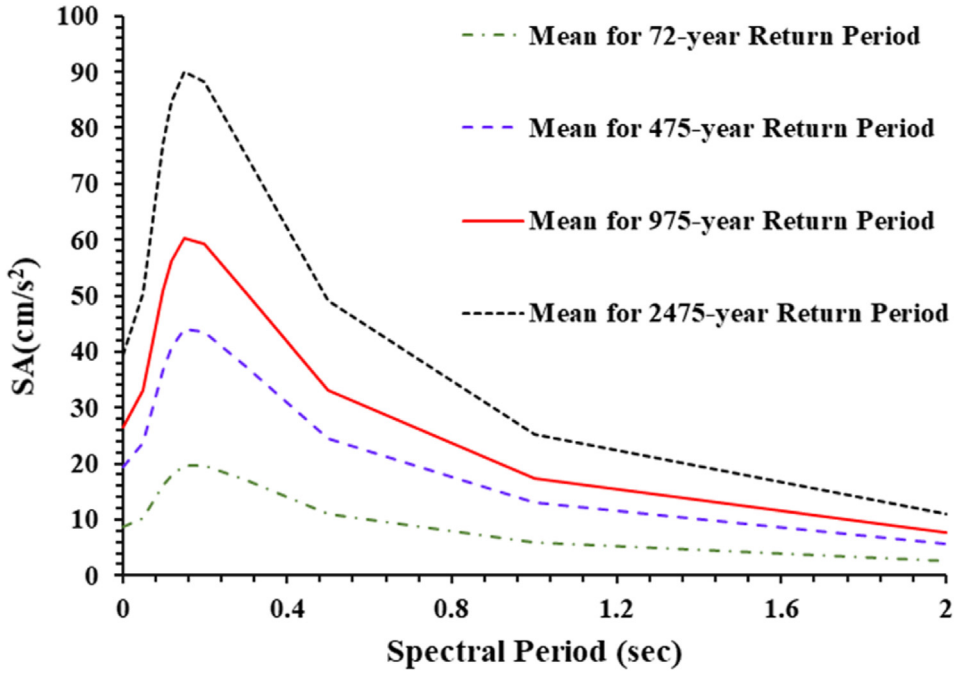

Figure 24. Unified hazard spectra for the rock sites of 72, 475, 975 and 2475 years return period in Sanaa city.

was based on IBC [25] and ASCE 7–16 [26] (Recommended Provisions for Seismic Regulations for New Buildings and Other Structures - NEHRP). The shear wave velocity (v_s(ft/sec)) for type B soil is $2500 < v_s \leq 5000$ [26]. Type B soil is cohesive and has often been cracked or disturbed, with pieces that do not stick together, similar to Type A soil. Type B soil has medium unconfined compressive strength between 0.5 and 1.5 tons per square foot. Examples of Type B soil include angular gravel, silt, silt loam, and soils that are fissured or near sources of vibration but can otherwise be Type A. If the soil differs from that of B, the code coefficients are used to convert the S_s and S_1 values into values that are compatible with the type of this different soil.

7. Results

The findings of the PSHA in Yemen were processed to obtain the mean acceleration value at each location. An estimated UHS for each location on the hazard maps over the range of periods relevant for popular engineering structures was produced. The PGA and 5% damped horizontal spectral acceleration values at 0.2 and 1 s SA were mapped. The seismic hazard maps of Yemen show the overall average ground motion in cm/s^2 for a rock condition. This value represents the distribution of ground motion over a 50-year period with 10% and 2% probabilities of exceeding in 475 and 2475 years (return periods), respectively (Figures 16, 17, 18, 19, and 20).

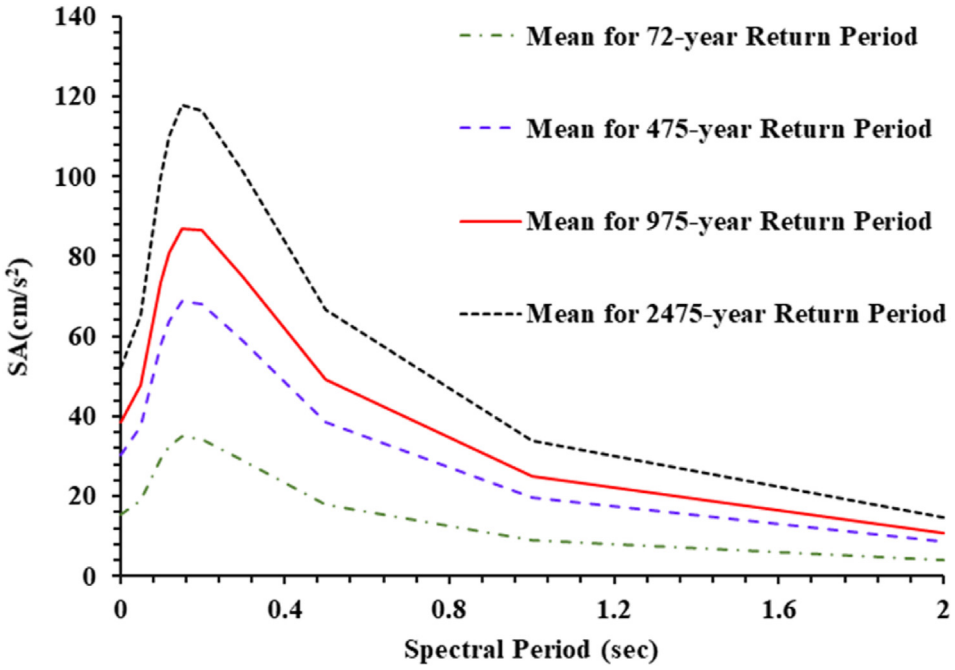

Figure 25. Unified hazard spectra for the rock sites of 72, 475, 975 and 2475 years return period in Dhamar city.

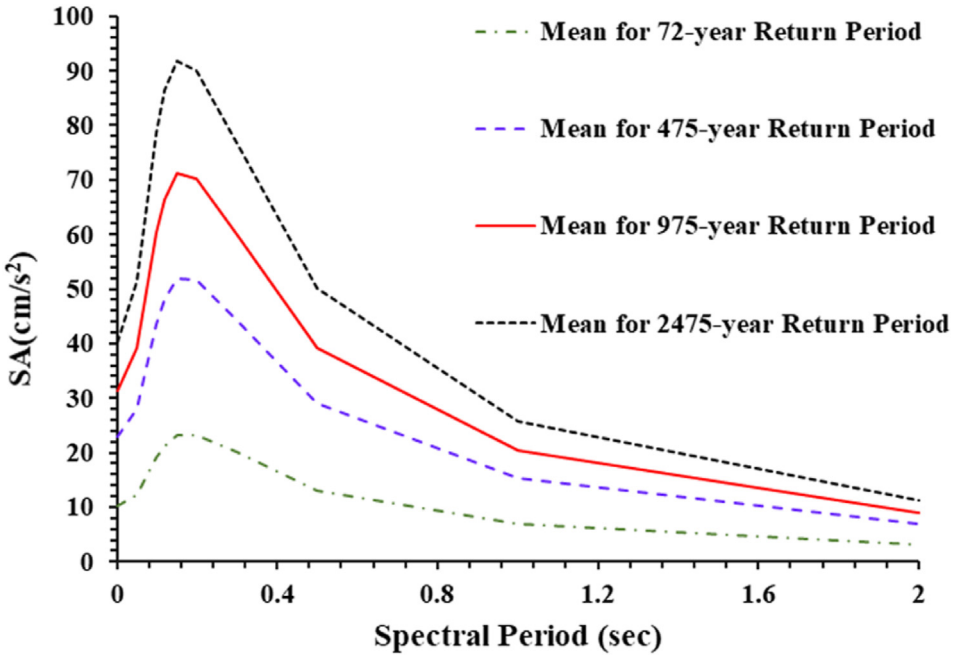

Figure 26. Unified hazard spectra for the rock sites of 72, 475, 975 and 2475 years return period in Aden city.

Dhamar area has the greatest seismic hazard in Yemen in accordance with seismic hazard maps and the high seismic activity inside the region. The second active area is in the Sana'a region and its surrounding northern regions. In the southern part of Yemen, moderate seismic activity has been detected near Aden. Some areas have experienced relatively similar seismic activity to their surroundings, such as Yemen's west and south coasts, Abyan region, Taiz region, Dhale region, and Lahij region. Acceleration values throughout the Eastern Desert Shabwah, Sayun, and Almahrah are characterized by extremely low seismic activity, as shown in Figures 16, 17, 18, 19, and 20.

The results of the present research are compared to those of Yemen's neighboring nations, Saudi Arabia and Oman, who have seismic hazard assessment programs of their own. Our results are mostly similar to those of the SBC map, which indicates modest hazard levels in the Sa'dah region and in Almahrah, which is close to the Oman border. A detailed PSHA is conducted for some of Yemen's most important cities, including Sana'a, Dhamar, and Aden, because they are socioeconomically significant. As shown by the estimated seismic hazard curves for each seismic source in Sana'a, the Dhamar region has the largest effect on the Sana'a area. The Gulf of Aden Zone (zone No. 3) and intermediate depth earthquakes that occur in the Red Sea have a significant impact on the

Table 7. Estimated probabilistic seismic hazard for the center of Yemen cities with return periods of 475 and 2475 years.

Major city	475-year return period PGA (in g)	2475-year return period SA (in g)	
		S_S (0.2 s)	S_1 (1.0 s)
Sana'a	0.21	0.83	0.26
Al-Bayda	0.18	0.83	0.25
Al-Hudaydah	0.22	0.84	0.24
Al-Jawf	0.19	0.84	0.25
Al-Mahwit	0.20	0.83	0.24
'Amran	0.20	0.83	0.24
Dhamar	0.29	1.10	0.33
Hajjah	0.21	0.84	0.24
Ibb	0.24	0.89	0.25
Ma'rib	0.19	0.89	0.26
Raymah	0.21	0.84	0.24
Sa'dah	0.18	0.74	0.20
Taiz	0.22	0.87	0.24
Aden	0.23	0.89	0.24
Abyan	0.23	0.89	0.24
Dhale	0.22	0.90	0.27
Al-Mahrah	0.04	0.20	0.10
Hadramaut, Al-Mukalla	0.18	0.80	0.20
Hadramaut, Sayun	0.04	0.15	0.07
Shabwah, Ataq	0.09	0.15	0.06
Lahij	0.23	0.87	0.24

city of Aden. PGA and SA values in 21 Yemeni main cities are shown in Table 7 for return periods of 475 and 2475 years.

The PGA results for this study are compared with previous studies for some locations (Table 8). For SA values at 0.2 and 1.0 s spectral periods, the current study is the first for the Yemen region, distinguishing it from previous studies. A difference is observed between the PGA values estimated in our study and those obtained in previous studies. The discrepancy may be explained by certain limitations and inadequacies in previous studies, such as the use of the logic tree method and attenuation relations. The current study is based on a probabilistic method to seismic hazard assessment that considers all of the contributing characteristics of the seismic source and attenuation relation utilized for SBC. Some findings vary significantly from prior research, especially for Dhamar City, and the present study is similar to Dhamar City in a previous study of Al-Raziqi et al. (2012) [52].

8. Conclusion

In this study, seismic hazard maps were created and used for seismic zoning, which corresponds to the code currently used in Yemen IBC [25] and when a Yemen seismic building code is created in the future. The authors provide maps with return periods of 475 and 2,475 years that illustrate horizontal PGA and 0.2 and 1.0 s SA for rock site conditions, where civil engineers and structural engineers are particularly interested in this spectral period in their structural designs. Uncertainties in seismic source, maximum magnitude, and ground motion models were integrated into the seismic hazard model by using a logic tree approach. The research indicates that the seismic hazard in most of Yemen is low to moderate, and that seismic design may not be needed for normal engineering buildings, with the exception of Dhamar City. The UHS for Sana'a, Dhamar, and Aden are calculated. The generated UHS curves for Sanaa, Dhamar, and Aden show seismic hazard in terms of building height, accurately reflecting real levels of hazard at all frequencies. Combining the existing results with site-specific variables is essential to derive seismic design coefficients for the significant buildings.

As a consequence of the study, the findings will be used as the main input for further research into seismic risk in Yemen, which results in probabilistic or deterministic estimations of property and life loss.

Declarations

Author contribution statement

Mohammed Alrubaidi: Conceived and designed the experiments; Performed the experiments; Analyzed and interpreted the data; Contributed reagents, materials, analysis tools or data; Wrote the paper.

Mohammed S. Alhaddad: Conceived and designed the experiments; Performed the experiments; Analyzed and interpreted the data.

Sulaiman I. H. Al-Safi & Alhammadi, S. A: Performed the experiments; Contributed reagents, materials, analysis tools or data; Wrote the paper.

Abobaker S. Yahya & Aref A. Abadel: Contributed reagents, materials, analysis tools or data; Wrote the paper.

Funding statement

This work was supported by the Deanship of Scientific Research at Princess Nourah Bint Ab-dulrahman University through the Fast-track Research Funding Program.

Table 8. Comparison between the present study results of PGA (475-year return periods), and previous studies.

Major city	Thenhaus et al. 1983 [53] (cm/sec^2)	AL-Haddad et al. 1994 [7] (cm/sec^2)	Al-Amri 1995 [54] (cm/sec^2)	AL-Dafiry 2004 [3] (Factor-Z)	Al- Suba'i 2008 [5] (cm/sec^2)	Mohindra et al. 2012 [6] (cm/sec^2)	Current study (cm/sec^2)
Sana'a	23	20	20	0.3	17	24	21
Al Bayda	*n/a*[*]	20	*n/a*	0.3	18	5	18
Al Hudaydah	20	20	*n/a*	0.3	19	24	22
Dhamar	22	20	*n/a*	0.3	17	19	29
Ibb	*n/a*	20	*n/a*	0.3	16	15	24
Ma'rib	*n/a*	20	*n/a*	0.2	18	20	26
Sa'dah	21	17	12	0.3	20	13	18
Aden	*n/a*	20	*n/a*	0.3	17	29	23
Al Mahrah	*n/a*	5	*n/a*	0.3	*n/a*	10	4
Al Mukalla	*n/a*	25	*n/a*	0.3	*n/a*	14	18

[*] Where *n/a*: this city not included in the previous study.

Data availability statement

Data included in article/supplementary material/referenced in article.

Declaration of interests statement

The authors declare no conflict of interest.

Additional information

No additional information is available for this paper.

References

[1] Hani M. Zahran, et al., On the development of a seismic source zonation model for seismic hazard assessment in western Saudi Arabia, J. Seismol. 20 (3) (2016) 747–769.
[2] CRISIS2007 M. Ordaz, A. Aguilar, J. Arboleda, Program for Computing Seismic hazard, Instituto de Ingeniería, Universidad Naconal Autónoma de México, UNAM, México, 2007.
[3] AL-Dafiry, A. Hamoud, " AL-Dafiry, Map for earthquake zones of Yemen republic to Be used in the design of different constructions" journal of engineering science, Assiut Univ. 33 (1) (Jan. 2005) 43–59. Egypt.
[4] Uniform Building Code, International Building Code, International Code Council, USA, 1997.
[5] K.A. Al-Suba'i, Seismic hazard assessment of the western Yemen region, J. Sci. Technol. 13 (2008).
[6] R. Mohindra, A.K. Nair, S. Gupta, U. Sur, V. Sokolov, Probabilistic seismic hazard analysis for Yemen, Int. J. Geophys. (2012 Jan 1) 2012.
[7] M. Al-Haddad, G.H. Siddiqi, R. Al-Zaid, A. Arafah, A. Necioglu, N. Turkelli, A basis for evaluation of seismic hazard and design criteria for Saudi Arabia, Earthq. Spectra 10 (2) (1994 May) 231–258.
[8] H.M. Zahran, S.M. El-Hady, Seismic hazard assessment for Harrat Lunayyir–A lava field in western Saudi Arabia, Soil Dynam. Earthq. Eng. 100 (2017 Sep 1) 428–444.
[9] H.M. Zahran, V. Sokolov, S. El-Hadidy, Deterministic seismic hazard assessment for the Makkah region, western Saudi Arabia, Arab. J. Geosci. 12 (15) (2019 Aug) 1–5.
[10] V. Sokolov, H.M. Zahran, S.E. Youssef, M. El-Hadidy, W.W. Alraddadi, Probabilistic seismic hazard assessment for Saudi Arabia using spatially smoothed seismicity and analysis of hazard uncertainty, Bull. Earthq. Eng. 15 (7) (2017 Jul) 2695–2735.
[11] Y. Al-shijbi, I. El-Hussain, A. Deif, A. Al-Kalbani, A.M. Mohamed, Probabilistic seismic hazard assessment for the Arabian Peninsula, Pure Appl. Geophys. 176 (4) (2019 Apr) 1503–1530.
[12] V. Sokolov, H.M. Zahran, Seismic hazard analysis for development of risk-targeted ground-motion maps in the western Saudi Arabia, in: In Proceedings 16-th European Conference on Earthquake Engineering, Thessaloniki, Greece, 2018 Jun, pp. 18–21.
[13] F. Rehman, A.M. Alamri, S.M. El-Hady, H.M. Harbi, A.H. Atef, Seismic hazard assessment and rheological implications: a case study selected for cities of Saudi Arabia along the eastern coast of Red Sea, Arab. J. Geosci. 10 (24) (2017 Dec) 1–7.
[14] K. Abdelrahman, A.M. Al-Amri, N.A. Al-Otaibi, M. Fnais, E. Abdelmonem, Seismic hazard assessment of Al mashair area, makkah Al-mukaramah (Saudi Arabia), in: In Conference of the Arabian Journal of Geosciences 12, 2018 Nov, pp. 227–230. Springer, Cham.
[15] R. Jena, B. Pradhan, G. Beydoun, A. Al-Amri, H. Sofyan, Seismic hazard and risk assessment: a review of state-of-the-art traditional and GIS models, Arab. J. Geosci. 13 (2) (2020 Jan) 1–21.
[16] A.K. Abdelfattah, M.F. Abdelwahed, S. Qaysi, H. Alzahrani, Simulation of strong ground motions onshore the southeastern coast of the Red Sea, Saudi Arabia, J. Afr. Earth Sci. 184 (2021 Dec 1) 104373.
[17] J.P. Poirier, M.A. Taher, Historical seismicity in the near and Middle East, North Africa, and Spain from Arabic documents (VIIth-XVIIIth century), Bull. Seismol. Soc. Am. 70 (6) (1980 Dec 1) 2185–2201.
[18] N.N. Ambraseys, The Seismicity of Saudi Arabia and Adjacent Areas. Kingdom of Saudi Arabia, King Abdulaziz City for Science and Technology, 1988.
[19] N.N. Ambraseys, C. Melville, Evidence for intraplate earthquakes in northwest Arabia, Bull. Seismol. Soc. Am. 79 (4) (1989 Aug 1) 1279–1281.
[20] A.W. Sadek, Seismic map for the state of Kuwait, Emir. J. Eng. Res. 9 (2) (2004) 53–58.
[21] A.M. Al-Amri, T.A. Alkhalifah, Improving the level of seismic hazard parameters in Saudi Arabia using earthquake location and magnitude calibration, in: In Proceedings of the Third Symposium on Scientific Research and Technological Development Outlook in the Arab World, 2004 May.
[22] A. Rodgers, A.R. Fowler, A.M. Al-Amri, A. Al-Enezi, The March 11, 2002 Masafi, United Arab Emirates earthquake: insights into the seismotectonics of the northern Oman Mountains, Tectonophysics 415 (1-4) (2006 Mar 27) 57–64.
[23] A.M. Al-Amri, Seismic Zones Regionalization of the Arabian Peninsula, SSC – Technical Report, 2004 (4).
[24] I. El-Hussain, A. Deif, K. Al-Jabri, N. Toksoz, S. El-Hady, S. Al-Hashmi, K. Al-Toubi, Y. Al-Shijbi, M. Al-Saifi, S. Kuleli, Probabilistic seismic hazard maps for the sultanate of Oman, Nat. Hazards 64 (1) (2012 Oct) 173–210.
[25] Benjamin. Trombly, The International Building Code (IBC)." CMGT 564-Term Paper, 2018.
[26] American Society of Civil Engineers, Minimum Design Loads and Associated Criteria for Buildings and Other Structures, American Society of Civil Engineers, 2017.
[27] Al-khirbash, A. Salah, El-Anba'awy, E. Mohamed, Geology of Yemen, Obadi Studies & Publishing Center, Sana'a, Yemen, 1995.
[28] N.N. Ambraseys, M. Srbulov, Attenuation of earthquake-induced ground displacements, Earthq. Eng. Struct. Dynam. 23 (5) (1994 May) 467–487.
[29] M. Kassim, G. Heo, D.S. Kessel, A systematic methodology approach for selecting preferable and alternative sites for the first NPP project in Yemen, Prog. Nucl. Energy 91 (2016 Aug 1) 325–338.
[30] Al-Sinawi, A. Sahil, Al-Aydrus, A. Ahmed, Seismicity of Yemen, Obadi Studies & Publishing Center, Sana'a, 1999.
[31] United States Geological Survey (USGS). Earthquakes and plate tectonics. Earthquake Hazards Program, National Earthquake Information Center, World Data Center for Seismology, Denver, USA. https://www.usgs.gov/.
[32] European–Mediterranean Seismological Center (EMSC). www.emsc-csem.org.
[33] The International Seismological Centre (ISC). http://www.isc.ac.uk/.
[34] National Seismological Observatory Center (NSOC), Dhamar, Yemen.
[35] D. Giardini, G. Grünthal, K.M. Shedlock, P. Zhang, The GSHAP global seismic hazard map, Ann. Geophys. (6) (1999 Nov 25) 42.
[36] N.A. Abrahamson, J.J. Bommer, Probability and uncertainty in seismic hazard analysis, Earthq. Spectra 21 (2005) 603–607.
[37] A. Deif, K. Abou Elenean, M. El Hadidy, A. Tealeb, A. Mohamed, Probabilistic seismic hazard maps for Sinai Peninsula, Egypt, J. Geophys. Eng. 6 (3) (2009 Sep 1) 288–297.
[38] C.A. Cornell, Engineering seismic risk analysis, Bull. Seismol. Soc. Am. 58 (5) (1968 Oct 1) 1583–1606.
[39] R.K. McGuire, FORTRAN computer program for seismic risk analysis, US Geol. Surv. (1976).
[40] L. Reiter, Earthquake hazard Analysis, Columbia University Press, Columbia, 1990.
[41] H.A. Merz, Aftershocks in Engineering Seismic Risk Analysis, Doctoral dissertation, Massachusetts Institute of Technology, 1973.
[42] J.K. Gardner, L. Knopoff, Is the sequence of earthquakes in Southern California, with aftershocks removed, Poissonian? Bull. Seismol. Soc. Am. 64 (5) (1974 Oct 1) 1363–1367.
[43] A.M. Al-Amri, Seismotectonics and Seismogenic Source Zones of the Arabian Platform. InLithosphere Dynamics and Sedimentary Basins: the Arabian Plate and Analogues, Springer, Berlin, Heidelberg, 2013, pp. 295–316.
[44] S.A. Alsinawi, S.G. Baban, A.S. Issa, Historical Seismicity of the Arab Region. InProceedings of the Third Arab Seismological Seminar, Riyadh Saudi Arabia, 1986, pp. 11–33.
[45] B. Gutenberg, C.F. Richter, Frequency of earthquakes in California, Bull. Seismol. Soc. Am. 34 (4) (1944 Oct 1) 185–188.
[46] C.A. Cornell, E.H. Vanmarcke, The major influences on seismic risk, in: In Proceedings of the Fourth World Conference on Earthquake Engineering 1, 1969 Jan 13, pp. 69–83.
[47] D.H. Weichert, Estimation of the earthquake recurrence parameters for unequal observation periods for different magnitudes, Bull. Seismol. Soc. Am. 70 (4) (1980 Aug 1) 1337–1346.
[48] D.J. Shearman, G.P. Walker, B. Booth, N.L. Falcon, The geological evolution of southern Iran: the report of the Iranian Makran expedition, Geogr. J. (1976 Nov 1) 393–410.
[49] M.G. Bonilla, R.K. Mark, J.J. Lienkaemper, Statistical relations among earthquake magnitude, surface rupture length, and surface fault displacement, Bull. Seismol. Soc. Am. 74 (6) (1984 Dec 1) 2379–2411.
[50] D.L. Wells, K.J. Coppersmith, New empirical relationships among magnitude, rupture length, rupture width, rupture area, and surface displacement, Bull. Seismol. Soc. Am. 84 (4) (1994 Aug 1) 974–1002.
[51] T.C. Hanks, W.H. Bakun, A bilinear source-scaling model for M-log A observations of continental earthquakes, Bull. Seismol. Soc. Am. 92 (5) (2002 Jun 1) 1841–1846.
[52] A. Al-Raziqi, A. Al-Sanabani, A. Al-Aydrus, Assessment of geotechnical seismic hazard of the Dhamar city, Yemen, Egypt. J. Eng. Sci. Technol. 15 (2012) 244–255, 2012 Jun 1;15(EIJEST).
[53] P.C. Thenhaus, Summary of Workshops Concerning Regional Seismic Source Zones of Parts of the Conterminous United States Convened by the US Geological Survey 1979-1980, Golden, Colorado, Unknow, 1983.
[54] A.M. Al-Amri, Recent seismic activity in the northern Red Sea, J. Geodyn. 20 (3) (1995 Nov 1) 243–253.